DOI: 10.1002/ejic.201100516

Ruthenium Polypyridyl Sensitisers in Dye Solar Cells Based on Mesoporous TiO_2

Anna Reynal*[a] and Emilio Palomares*[a,b]

Keywords: Dye-sensitized solar cells / Ruthenium / Charge transfer / Sensitizers

At present, one of the most studied molecular device for the conversion of sunlight into electricity is the dye-sensitised solar cell (DSSC). To date, ruthenium polypyridyl complexes have shown the highest light-to-energy conversion efficiencies because of their photophysical, photochemical and electrochemical properties. In addition, the overall efficiency achieved by DSSCs is strongly dependent on the interfacial charge-transfer reactions that take place between the different components of the solar cell: the injection of electrons into the conduction band of the semiconductor by the dye, the transport of electrons through the semiconductor towards the working electrode contact, dye regeneration by the redox pair present in the electrolyte and the recombination reaction between the photoinjected electrons in the semiconductor and the oxidised species of the dye and the electrolyte. This microreview comprises: (i) the operational principles of complete functional photovoltaic devices and (ii) several synthetic methods, properties and main applications of most relevant homoleptic and heteroleptic ruthenium complexes reported in the literature.

Introduction

The world primary energy consumption has already surpassed 6×10^{20} J, and this is expected to increase in the future as a result of population and economic growth.[1] The principal energy supply to meet the energy needs of our planet comes from liquid fuels, coal and natural gas. However, the non-renewable nature of fossil fuels, in addition to the high emissions of CO_2 into the atmosphere when they are used has made them an important issue in the last two decades.[1,2] For this reason, the search for sustainable, clean and secure energy source is a must if we are aiming to keep our lifestyle and ensure a future for coming generations. From a wide range of possible alternatives we foresee that solar, wind and biomass are the most suitable alternatives to fossil fuels. In fact, our planet receives a huge amount of energy from sunlight (4.3×10^{20} J in 1 h), and, therefore, it seems perfectly logical to consider solar energy as the most likely possible renewable energy resource that could be exploited in the future either by direct conversion into electrical power or by transformation into useful fuels.[3] In this microreview, we will focus only on the light-to-electrical power generation, although we are aware of the

[a] Institute of Chemical Research of Catalonia (ICIQ), Avda. Paisos Catalans, 16, 43007 Tarragona, Spain
Fax: +34-977920823
E-mail: epalomares@iciq.es
[b] Institució Catalana de Recerca i Estudis Avançats (ICREA), Passeig Lluís Companys, 23, 08010 Barcelona, Spain

Anna Reynal finished her Bachelor studies in Chemistry at the University of Girona (Spain) in 2006 and received her Master's degree in Nanoscience and Nanotechnology at the University Rovira i Virgili (Spain) in 2007. In 2010, she finished her doctoral studies under the supervision of Emilio Palomares on the topic "Ruthenium polypyridyl complexes as photosensitisers for molecular photovoltaic devices: Influence of the dye structure and the presence of additives to the device performance". Her scientific career is now focused on the study of molecular catalysts and nanostructured materials for the photochemical reduction of CO_2 to fuels at Imperial College London (United Kingdom).

Emilio Palomares (Valencia, Spain. 1974) graduated from the University of Valencia (Spain) in 1997 (B.Sc. Biology). He obtained his Ph.D. in 2001, at the Universidad Politécnica de Valencia (Spain) under the supervision of Prof. Hermenegildo García. He was awarded a Marie Curie Fellowship to work as a Post-Doctoral Fellow at the Centre for Electronic Materials and Devices of Imperial College London (United Kingdom). He returned to Spain in 2004 after being awarded a Ramon y Cajal Fellowship to work at the Institute of Molecular Science at the University of Valencia (Spain). In 2006, he took a position at ICIQ as independent researcher, where he currently leads a research group focused on molecular and biomolecular devices for energy production. In 2007, he was appointed ICREA (Catalan Institution of Research and Advanced Studies) Professor. Professor Palomares has several awards including the Young Chemist Research Award of the Real Sociedad Española de Química and he is Fellow of the European Research Council (ERC Starting Grant). Prof. Palomares has published more than 100 peer-reviewed research papers.

increasing attention that light-to-fuel conversion devices are attracting.

Nowadays, the majority of efficient and commercial photovoltaic devices are based on semiconductor p-n junction solar cells; however, many other systems and materials have been developed in order to improve the efficiency or reduce the total cost of photovoltaic converters.[4] One of the most studied so called "alternative" systems is the dye-sensitised solar cell based on mesoporous TiO_2. Since the key publication of the principles of operation of this molecular photovoltaic device,[5] the study and improvement of this kind of energy converter has attracted the attention of numerous scientific groups including our own.[6] DSSCs are based on the absorption of light by the photosensitiser, and the most used and efficient dyes are based on ruthenium polypyridyl complexes. The well-known and easily tunable photophysical, photochemical and electrochemical properties of these dyes make them excellent candidates for light-harvesting systems in energy conversion devices.[7] We have structured this microreview following a logical description of (i) the operational principles of DSSCs, (ii) the fundamental parts of the device and (iii) a description of the most representative ruthenium sensitisers used for DSSCs.

Operating Principles of Dye-Sensitised Solar Cells

DSSCs are regenerative photoelectrochemical cells based on the sensitisation of a nanocrystalline semiconductor with a dye able to absorb a wide range of the solar spectrum.[8] The most widely used semiconductor in the working electrode of a DSSC is TiO_2, which is supported onto transparent fluorine-doped tin oxide (FTO) conducting glass. The counter electrode consists of a layer of platinum coated on FTO conducting glass. The two electrodes are sealed with a polymer, and the cell is completed with a redox electrolyte (Figure 1).

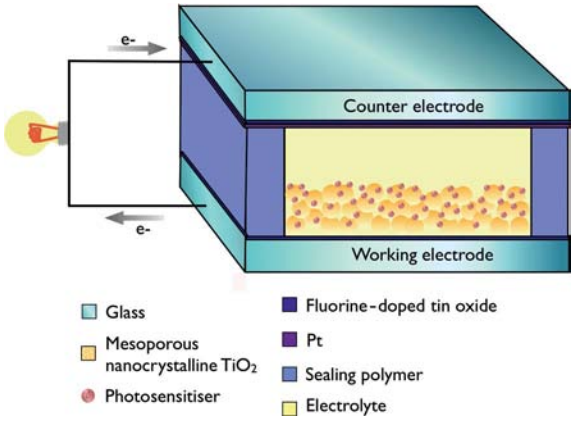

Figure 1. Schematic representation of the cross-section of a DSSC.

Figure 2 shows a schematic representation of the charge-transfer reactions occurring in a DSSC. Upon absorption of sunlight [Equation (1)], the photosensitiser promotes an electron from its ground state to the excited state, which corresponds to the metal-to-ligand charge-transfer transition (MLCT) of the dye when Ru^{II} polypyridyl dyes are used.

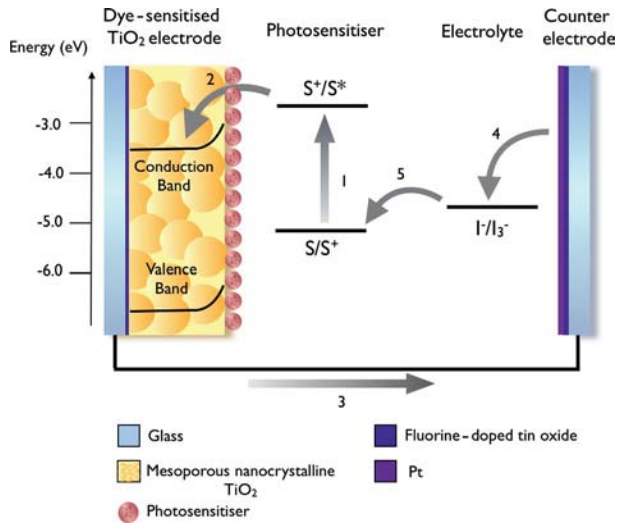

Figure 2. Scheme showing the operating principle and energy level diagram of a dye-sensitised solar cell. S, S^+, S* represent the photosensitiser in the ground, and the oxidised and excited states, respectively. (1) Photoexcitation of the dye, (2) electron injection from the dye excited state to the semiconductor, (3) external circuit, (4) regeneration of the electrolyte and (5) regeneration of the oxidised dye.

$$\text{Photoexcitation: } S + h\nu \rightarrow S^* \quad (1)$$

This electron is subsequently injected into the conduction band of the semiconductor [Equation (2)], which arrives at the back contact and flows through an external circuit to the counter electrode. At the counter electrode, electrons are transferred to the redox pair present in the electrolyte. The most commonly used electrolyte contains the I^-/I_3^- redox couple, and at the counter electrode, triiodide is regenerated to iodide [Equation (3)]. Other electrolytes based on cobalt complexes have also been used with efficiencies that are catching up to the above-mentioned redox couple.[9] Finally, the cycle is completed with the regeneration of the oxidised dye by electron donation from the electrolyte [Equation (4)].

$$\text{Electron injection: } S^* + TiO_2 \rightarrow S^+ + e^-\text{-}TiO_2 \quad (2)$$

$$\text{Electrolyte regeneration: } I_3^- + 2e^- \rightarrow 3I^- \quad (3)$$

$$\text{Oxidised dye regeneration: } 2S^+ + 3I^- \rightarrow 2S + I_3^- \quad (4)$$

The regenerative cycle of dye-sensitised solar cells is based on reversible reactions, and the devices can convert sunlight into electricity without suffering permanent chemical transformations.

However, this system has undesirable loss mechanisms, which decrease the total efficiency of the device (Figure 3). The three main loss reactions observed are (a) deactivation of the dye excited state [Equation (5)], (b) recombination of the photoinjected electrons in the semiconductor with the

oxidised photosensitiser [Equation (6)], and (c) recombination of the photoinjected electrons in the semiconductor with the oxidised form of the redox mediator [Equation (7)]. The latter recombination reaction is also called "dark current".

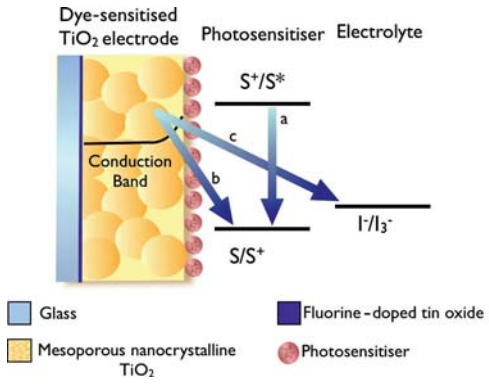

Figure 3. Scheme of the loss reactions occurring in a DSSC. (a) Dye excited state deactivation, (b) e^--TiO_2/S^+ back electron transfer, and (c) e^--TiO_2/I_3^- recombination reaction.

Dye excited state deactivation: $S^* \rightarrow S$ (5)

Back electron transfer: e^--$TiO_2 + S^+ \rightarrow TiO_2 + S$ (6)

$I_3^- + 2e^-$-$TiO_2 \rightarrow 3I^- + 2TiO_2$ (7)

Despite the loss processes that occur in DSSCs, the reason for the high light-energy conversion efficiencies observed in optimised devices is due to the rather favourably balanced kinetic competition, which ensures forward electron-transfer reactions dominate over the loss processes mentioned. For most dyes, loss reactions are several orders of magnitude slower than the forward processes when the devices are working under normal operating conditions, which enables efficient charge separation, charge transport and charge collection to occur (Table 1).[10]

Fundamental Constituents of Dye-Sensitised Solar Cells

DSSCs are devices composed of multiple components, and their overall efficiency depends strongly on the individual properties of each constituent. Great efforts have been made towards the optimisation of the materials, such as the semiconductor metal oxide, the photosensitiser, the electrolyte and the counter electrode, used in the fabrication of solar cells.

The Working Electrode (WE)

As mentioned before, in DSSCs, a wide band gap semiconductor material, such as TiO_2, is used at the working electrode. TiO_2 is only able to absorb UV light (Figure 4), and, therefore, its photon-to-current efficiency is rather low. The sensitisation of the metal oxide with a dye leads to an increase in the absorption range. Yet, the dye must be able to "charge" the semiconductor film by injecting electrons into the metal oxide conduction band.[11] At the working electrode, we also find deposited onto the transparent glass a highly conductive metal oxide as selective contact. In most cases such a metal oxide is fluorine-doped tin oxide (Figure 1). Although other metal oxides such as tin-doped indium oxide (ITO) present higher conductivities, its thermal instability strongly increases the resistance of the material when the glass is exposed to high temperatures over a long period of time.

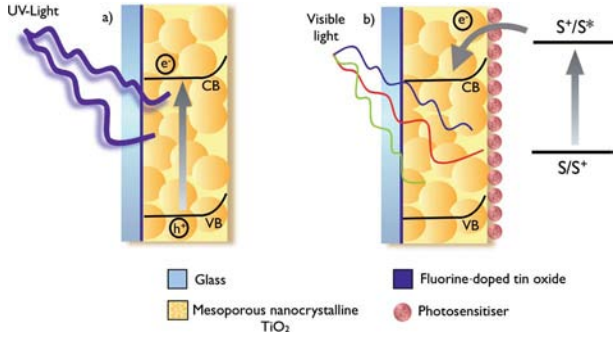

Figure 4. Schematic representation of (a) the formation of an exciton in a semiconductor by the absorption of UV light, and (b) electron injection into the conduction band of a semiconductor by the absorption of visible light by a photosensitiser.

Four important processes take place at the WE: (i) light harvesting, (ii) subsequent charge separation, (iii) electron transport and (iv) electron recombination reactions. Light harvesting is performed by the chromophore, which consists of a molecular photosensitiser. Charge separation occurs at the interface between the dye and the semiconductor, and

Table 1. Timescales of forward and loss processes occurring in DSSCs.

Forward processes	Loss processes
Electron injection from the dye excited state into the semiconductor conduction band (10^{-10}–10^{-9} s)	Excited state deactivation ($>10^{-9}$ s)
Dye regeneration by the redox electrolyte (10^{-9}–10^{-6} s)	Back electron transfer from the photoinjected electrons into the TiO_2 conduction band to the oxidised dye (10^{-6}–10^{-3} s)
Electron transport through the TiO_2 nanoparticles towards the back contact of the electrode	Electron recombination between the photoinjected electrons into the TiO_2 conduction band and the electrolyte (10^{-3}–10^{1} s)

the electron travels through the TiO_2 and the hole through the electrolyte. This is the key point in these devices, as charges with opposite sign are not transported through the same material as in silicon-based solar cells. Electron recombination also takes place at the interface between the surface of the semiconductor and the dye or the electrolyte.

The TiO_2 semiconductor thin film in DSSCs is deposited in the form of mesoporous crystalline nanoparticles. The most important characteristics of a TiO_2 film that have to be optimised are the surface area, the porosity, light scattering and electron diffusion.[12]

The semiconductor must have a large surface area in order to anchor sufficient dye to achieve a near 100% light harvesting, which is obtained with the preparation of small TiO_2 nanoparticles. The size of the nanoparticles also affects the size of the pores and the light scattering properties of the film. The porosity of the film has to be optimised in order to allow electrolyte penetration through the thickness of the film and ensure fast dye regeneration. Furthermore, the level of porosity has to be controlled in order to have enough interparticle connectivity so that electrons can diffuse through the film and reach the working electrode. The thickness of the film (d, cm) is also a key parameter to reach high conversion efficiencies, since charges at the back contact can only be collected if the thickness of the film is lower than the electron diffusion length (L_n, cm) [Equations (8) and (9)]. L_n is defined as the distance that the electron can travel before recombining with an electron acceptor,[13] and it is dependent on the electron diffusion coefficient (D_e, $cm^2 s^{-1}$) and the lifetime of the electron (τ_e, s).

$$L_n > d \tag{8}$$

$$L_n = \sqrt{D_e \cdot \tau_e} \tag{9}$$

The diameter of the nanoparticles is in the range 10–25 nm, large enough in order not to exhibit important quantum size effects. For this reason, the semiconductor film can be considered as a network composed of bulk nanocrystals.

At a first glance, the properties of mesoporous nanocrystalline films would seem disadvantageous relative to their compact single-crystal analogues because (i) the electrolyte penetrates into the pores of the semiconductor producing a huge junction contact area, which increases the probability of electron/hole recombination, (ii) the inherent conductivity of the film is very low, (iii) the multiple traps present in the film decrease the electron diffusion coefficient[14] and (iv) the small size of the nanoparticles in contact with the electrolyte restricts the amount of electrical field a particle can support. However, such disadvantages are offset by the optical transparency of the nanoparticles and the enormous surface area of the films, which allows an extremely large number of photosensitiser molecules to be adsorbed onto the surface of the semiconductor.

The Molecular Sensitiser

Characteristics of Molecular Sensitisers

The function of the photosensitiser in DSSCs is (i) to absorb light in a wide range of the solar spectrum (Figure 5), (ii) to inject electrons into the conduction band of the semiconductor and (iii) to reduce the recombination between the photoinjected electrons at TiO_2 and the oxidised electrolyte. For all these reasons, the design of the dye has been tuned to fulfill several structural, photophysical and electrochemical requirements.[15]

The solar radiation conditions are defined by the air mass (AM) value. Air mass zero (AM-0) corresponds to the radiation that a device receives in the absence of an atmosphere between the light source and the solar cell. However, the extraterrestrial solar spectrum is different from the sunlight spectrum that arrives at the surface of the earth as a result of light scattering and absorption by H_2O, H_2, O_2, CO_2, O_3 and other species present in the atmosphere. Furthermore, the incident light falling on solar devices can be irradiated in the form of direct light, which comes straight from the sun, or in a diffuse form, which is light reflected off clouds, the ground or other objects. For this reason, AM-1.5G is defined as the corrected solar spectrum, including both direct and diffuse radiation, by considering the sun at an angle of 48.19°. Although the solar flux is 982 $W m^2$, it has been standardised to 1000 $W m^2$.

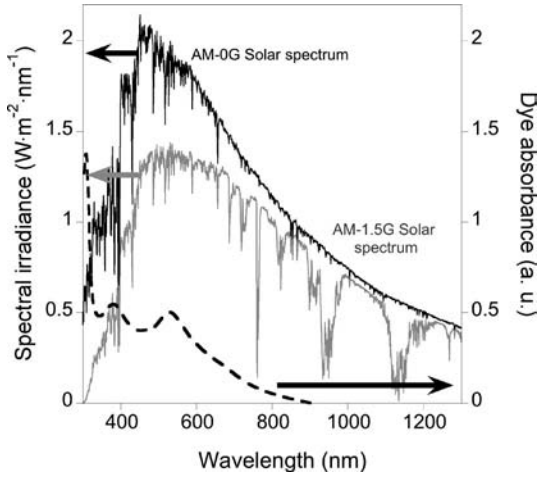

Figure 5. AM-0G solar spectrum (solid black), AM-1.5G solar spectrum[16] (solid grey) and absorption spectrum of *cis*-dithiocyanato-bis(4,4′-dicarboxy-2,2′-bipyridine)ruthenium(II) dye (dashed black).

In addition, the dye structure has to include one or more anchoring groups in order to bind strongly to the surface of the semiconductor and ensure a quantitatively efficient electron injection. Photosensitisers can interact with the surface of metal oxides through covalent bonds, hydrogen bonding, electrostatic interactions, hydrophobic interaction, van der Waals forces or entrapment inside the pores.[17] However, the formation of covalent bonds between the hydroxy groups present on the semiconductor nanoparticle surface and the different anchoring groups of the dyes in-

creases the amount of absorbed dye, the stability of the cell and the strength of the electronic coupling between the π* molecular orbital of the dye and the orbitals of TiO_2 and decreases the rate of dye desorption.[18] Although most of the sensitisers are linked to the semiconductor surface through carboxylic acid groups, a variety of different groups such as phosphonic acid,[19] boronic acid,[20] silanes[21] and other derivatives or moieties have been used.[22] The attachment of dyes through carboxylic acid groups is reversible, and the sensitisers can be desorbed from the films under basic conditions. Furthermore, several binding modes of a carboxylic acid group to the surface of a metal oxide are possible depending on the dye structure, the crystalline form of the metal oxide and the surface environment (Figure 6).[23]

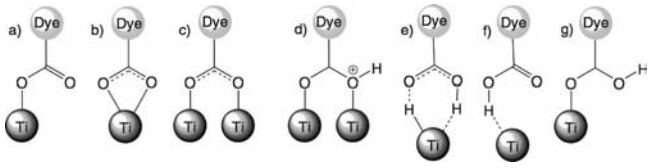

Figure 6. Possible binding modes of a carboxylic acid group to TiO_2. (a) Ester linkage, (b) chelate binding, (c, d) bidentate bridges, (e, f) hydrogen-bonding interactions and (g) monodentate binding through CO.

The redox properties of the dyes are also important for efficient charge separation. The dye excited state energy level must have higher energy than the conduction band of the semiconductor in order to be able to inject electrons into TiO_2, and the ground state must be sufficiently low to permit fast electron regeneration from the electrolyte redox couple. The HOMO–LUMO gap (HOMO: highest occupied molecular orbital, LUMO: lowest unoccupied molecular orbital) should be about 1.5 eV for optimum absorption of sunlight. Furthermore, the spatial orientation of the ground state and the excited state influences not only electron injection of the dye into the semiconductor conduction band and photosensitiser regeneration but also electron recombination between the photoinjected electrons into TiO_2 and the oxidised dye.[24] The LUMO should be in close contact with the semiconductor surface, while the HOMO should be separated from the electrode surface.

Another chemical aspect of photosensitisers is their solubility in organic solvents. The dye should be soluble in a volatile solvent to permit their adsorption onto the surface of the semiconductor, but should not be desorbed by the electrolyte solution. Finally, the redox reactions involving the dyes must be reversible, and the stability of the photosensitisers should permit many oxidation/reduction cycles without decomposition of the molecules.

Classification of Molecular Sensitisers

Many different compounds have been investigated for solar cell applications. They can be divided into three major groups: metal-containing complexes,[25] organic dyes[26] and natural compounds.[27]

Mononuclear and polynuclear transition-metal complexes have been widely studied as photosensitisers (Figure 7).[28] Systematic optimisation of the dye components such as the introduction of different anchoring ligands or the insertion of different chromophoric groups has been tested in dyes based on different metal ions, such as Ru^{II},[29] Os^{II},[30] Pt^{II},[31] Re^{I},[32] Cu^{I}[33] or Fe^{II}.[34] However, the most used compounds by far in DSSCs are ruthenium complexes. The easily tunable redox and photophysical properties, and the extensively studied synthetic approaches to these complexes, which allow the sequential introduction of different ligands, make these compounds ideal candidates for semiconductor sensitisation.

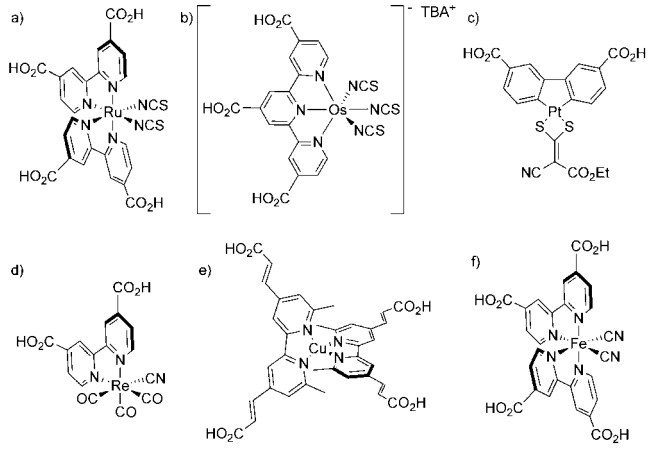

Figure 7. Molecular structures of metal-based sensitisers. (a) Octahedral Ru^{II} complex,[35] (b) octahedral Os^{II} complex,[36] (c) square-planar Pt^{I} complex,[31a] (d) octahedral Re^{I} complex,[32] (e) tetrahedral Cu^{II} complex[33b] and (f) octahedral Fe^{II} complex.[34a]

In addition to metal complex sensitisers, a wide range of organic dyes has been explored. This family of dyes offers several advantages relative to their metal-containing analogues, such as higher molar extinction coefficients, a large variety of different structures as chromophoric groups and the obvious fact that they do not contain precious metals such as Ru. Organic dyes such as porphyrins, phthalocyanines, perylenes, squaraines, conjugated donor–acceptor moieties, etc. have been explored (Figure 8) with varying success.[26,37] Although the efficiencies obtained with devices prepared with organic dyes are still lower than ruthenium-based DSSCs, recent publications have reported efficiencies of up to 10% with organic photosensitisers.[38] The main unfavourable characteristics of metal-free dyes are the narrow absorption bands, as in the case of phthalocyanines, which results in poorer sunlight harvesting, the tendency to form aggregates, alike perylenes, which prevent electron injection into the TiO_2 conduction band, and a lower stability relative to metal complexes such as the squaraines.

Natural photosensitisers (Figure 9) can also be used as dyes in molecular photovoltaic devices. Natural dyes are pigments extracted from plants, flowers and fruits that have been used mainly for educational purposes as a fast, low-cost and environmentally friendly source for the prepara-

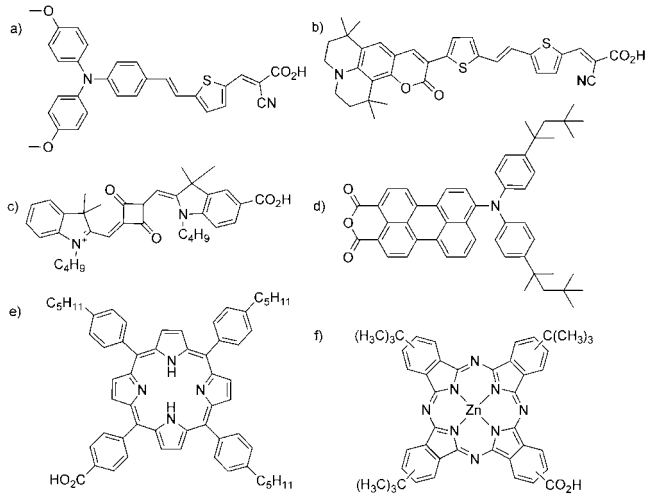

Figure 8. Molecular structures of a series of organic dyes. (a) Donor–π-acceptor dye with a triphenylamine donor moiety,[39] (b) donor–π-acceptor dye with a coumarin donor moiety,[40] (c) squaraine dye,[41] (d) perylene dye,[42] (e) porphyrin dye[43] and (f) phthalocyanine dye.[44]

tion of DSSCs. The most studied dyes are anthocyanins, but the overall efficiencies of this kind of dye are generally much lower than organic or metal complex sensitisers.

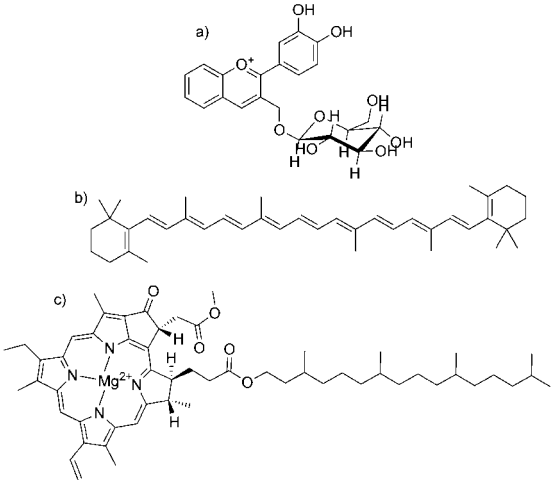

Figure 9. Molecular structures of natural dyes used in DSSCs. (a) Cyanin dye,[27] (b) β-carotene dye[45] and (c) chlorophyll dye.[46]

The Electrolyte

The electrolyte is the hole transporting material that fills the TiO_2 nano- and mesopores. There are three different kinds of hole transport materials employed in DSSCs: liquid electrolytes (we include here the electrolytes in which the redox mediators are dissolved in organic solvents, water or electrolytes composed of ionic liquids), quasi-solid-state electrolytes and solid electrolytes.[47]

However, in all these cases, the electrolyte must have a high conductivity to permit fast electron transfer from the counter to the working electrodes and efficient dye regeneration. For the same reason, the ionic species present in the electrolyte must have a high diffusion coefficient. The electrolyte should also be thermally, optically, chemically and electrochemically stable to avoid dye degradation or desorption from the metal oxide surface. Furthermore, the redox mediator should have adequate redox potentials to allow efficient dye regeneration. It is important that the electrolyte does not absorb in the visible region of the spectra, since it would reduce light absorption by the sensitiser.

Organic Solvent Based Electrolytes

Up to now, the most efficient DSSCs are based on organic solvent electrolytes because of their low viscosity, fast ion diffusion and high percolation into the pores of the semiconductor.[48] This electrolyte contains a redox couple, ionic liquid components and additives dissolved in an organic solvent.

The most efficient redox couple for the regeneration of the oxidised dye is the iodide/triiodide couple. However, the two major issues regarding the use of I^-/I_3^- are the severe corrosion problems for the device-sealing materials, which causes difficulties in device sealing and stability, and the complicated electrochemistry arising from the two-electron redox couple. In addition, the triiodide shows partial absorption of visible light. Alternative redox mediators such as Br^-/Br_3^-,[49] $SCN^-/(SCN)_2$,[50] $SeCN^-/(SeCN)_2$,[51] ferrocene$^+$/ferrocene,[52] Co^{II}/Co^{III} complexes,[53] Cu^{I}/Cu^{II} complexes,[54] Ni^{III}/Ni^{IV} complexes[55] or thiolate/disulfide dimer derived from 2-mercapto-5-methyl-1,3,4-thiazole[56] have been tested in DSSCs. However, inferior device efficiencies have been obtained because of inefficient dye regeneration, mass transport limitations or high recombination rates. The most common counterions of the iodide/triiodide couple are imidazolium and lithium cations, which can also affect the performance of the solar cell. Small cations such as Mg^{2+}, Li^+, Na^+ or H^+ can penetrate into the pores of the nanoparticles to form an ambipolar ion$^+$/e$^-$ with the photoinjected electrons of the conduction band, which increases the transport velocity of electrons in the TiO_2 network.[57] On the other hand, relatively large molecules such as imidazolium cations can be adsorbed onto the surface of the semiconductor nanoparticles, forming a Helmholtz layer, which restricts the contact of triiodide with the electrons from the TiO_2 conduction band.[58]

Imidazolium salts can also be used as a source of iodide in organic solvent based electrolytes for DSSCs. The addition of imidazolium salts in organic solvent based electrolytes usually increases the ionic conductivity.[59] Furthermore, the use of different additives such as guanidinium thiocyanate has been extensively used in order to optimise DSSC performance.

Room-temperature ionic liquids are attractive candidates as nonvolatile solvents for electrolytes too.[60] They are formed from an aromatic or non-aromatic cation such as imidazolium, pyridinium or quaternary ammonium ions and are also use as source for iodide (Figure 10).[61] Ionic liquids possess good chemical and thermal stability, very

low vapour pressure, nonflammability, high ionic conductivity and wide electrochemical windows, which are very useful properties for long-lived electrochemical devices.[62] However, their high viscosity usually limits the transport of the redox shuttle components, which occurs by diffusion, and dye regeneration is therefore not as good as for organic solvent based electrolytes.

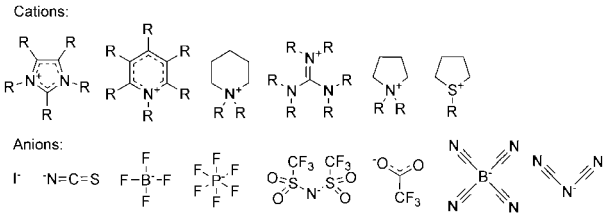

Figure 10. Molecular structure of the most commonly used cations and anions in ionic liquids. R corresponds to H, alkyl chains or other substituents.

Quasi-Solid-State Electrolytes

Quasi-solid-state electrolytes are gel-based materials with dispersed amounts of liquid electrolyte.[62] This type of electrolyte has the cohesive property of a solid electrolyte and the ion diffusion characteristics of a liquid electrolyte. Quasi-solid-state electrolytes are prepared by physical or chemical polymerisation of a gel, inorganic material or monomer that incorporates large amounts of liquid electrolyte.

Solid-State Electrolytes

Solid-state electrolytes can be divided into either hole transport materials (HTMs) or redox couple containing solid electrolytes. The first group requires a layer of an organic or inorganic large band gap HTMs to be deposited from solution or by vacuum deposition. Inorganic HTMs such as CuI, CuBr or CuSCN have been used in DSSCs but show low stability. On the other hand, one of the most used organic HTM is spiro-OMeTAD [2,2′-7,7′-tetrakis(*N*,*N*-di-*p*-methoxyphenylamine)-9,9′-spirobifluorene]. The solar cell mechanism with HTMs is equivalent to that with liquid or solid electrolytes: the oxidised dye is regenerated by the electrons from the HOMO energy level of the HTM instead of from the redox mediator for liquid electrolytes. At the same time, the HTM is reduced by the electrons that arrive at the counter electrode. However, the performance of DSSCs that use solid electrolytes is reduced because of low hole mobility, increased charge recombination between the semiconductor and the HTMs and low interfacial contact surface between the dye molecules and the solid electrolyte, which results from incomplete percolation of electrolyte into the pores of the nanoparticles. Redox-containing solid electrolytes incorporate a redox couple, usually I^-/I_3^-, as a transport medium in DSSCs in their polymeric structure. Although the efficiencies obtained with this kind of electrolyte are higher than with electrolytes based on HTMs, because of higher electron contact properties and lower charge recombination reactions, they are not as high as in liquid solvent based DSSCs.

The Effect of Additives

The maximum open circuit voltage of a DSSC is the difference in energy between the quasi-Fermi level of the semiconductor when illuminated and the redox potential of the electrolyte.[63] The V_{oc} is mainly affected by changes in the position of the conduction band edge of the semiconductor and by variations in the e^--TiO_2/electrolyte$^+$ recombination rate.

The conduction band of TiO_2 can be shifted by the presence of additives either in the electrolyte[64] or as coadsorbents,[65] or by exposing the cell to sufficiently high light intensities.

The composition of the electrolyte strongly affects the performance of DSSCs. Two main kinds of additives, adsorptive cations and nitrogen-containing molecules, can be intercalated between the TiO_2 nanoparticles or adsorbed onto their surface. The presence of these additives can affect electron injection, the open-circuit voltage, the electron-diffusion kinetics and the dye-regeneration rate. Cations such as Li^+, Na^+, Cs^+, K^+ or tetrabutylammonium$^+$ (TBA^+) charge the surface positively, which causes a downward shift of the conduction band position.[66] This effect increases the driving force for electron injection and improves the photocurrent, although the open-circuit voltage is reduced.[58,64b] On the other hand, ammonia and other nitrogen-containing heterocyclic molecules, such as 4-*tert*-butylpyridine (TBP),[67] can be adsorbed onto the surface of the semiconductor, which shifts the conduction band of TiO_2 upwards as a result of deprotonation of the TiO_2 surface. This leads to a negatively charged surface.[68] Nitrogen-containing molecules can also decrease electron recombination between the photoinjected electrons and the redox mediator by preventing the electrolyte from reaching the TiO_2 surface.

Coadsorbents, such as chenodeoxycholic acid (Cheno),[65a,69] are small molecules anchored onto the surface of the semiconductor together with the dye. They mostly consist of a hydrophobic chain and an anchoring group such as carboxylic acid or phosphonic acid, which can block exposed areas of TiO_2 that are not covered by photosensitisers. In addition to the barrier effect for e^--TiO_2/electrolyte$^+$, coadsorbents can shift the conduction band of the semiconductor down by protonating the TiO_2 surface.

The intercalation of coadsorbents between photosensitiser molecules can also prevent dye aggregation, an effect especially important in organic photosensitisers, which strongly reduces electron injection into the conduction band of the semiconductors.

The Counter Electrode (CE)

The counter electrode is the contact where the catalytic reaction to reduce the oxidised electrolyte occurs. For efficient DSSCs, the counter electrode should possess low resistance and a high rate of reduction of the redox mediator present in the electrolyte.[70]

The most widely used material as counter electrode is the highly transparent FTO conductive glass with a thin layer of platinum (<10-nm thick). Although different deposition techniques have been tested to create the molecular catalyst thin layer, thermal deposition of a Pt thin film shows more stability and a higher triiodide reduction rate.[71]

Different materials have been used as low-cost alternative materials to the platinum coated counter electrode. Metal substrates such as steel or Ni have been tested as molecular catalysts. However, the I^-/I_3^- redox species present in the electrolyte are corrosive towards these metals. The stability of these metallic counter electrodes can improve with the deposition of a Pt coating.[72] Carbon materials such as graphite or black carbon have also been tested. High efficiencies have been obtained with thick layers of carbon, because of the high surface contact area with the redox mediator but still far from the Pt layer.[73] Conducting polymers have also been used as counter electrodes, which allows the preparation of flexible devices; however, the device efficiency and stability have not reached the values obtained with standard iodine/iodide electrolyte in combination with the Pt counter electrode.

Ruthenium Polypyridyl Complexes as Ideal Sensitisers for Molecular Photovoltaic Devices

Ruthenium was discovered in 1844 in Tartu, Estonia, by Karl Karlovich Klaus, who named this new metal *Ruthenia*, the Latin name for Russia.[74]

Ruthenium, just like osmium, is a unique metal due to its ability to form complexes that cover the widest range of oxidation states theoretically allowed for a transition metal: from 8 in $[RuO_4]$ to –2 in $[Ru(CO)_4]^{2-}$; the most common are the Ru^{II} and Ru^{III} oxidation states.[75] The kinetic stability of the ruthenium complexes formed in a broad range of oxidation states, the reversible nature of most of their redox pairs and the wide range of well-known synthetic reactions for their preparation make these complexes very attractive for use in a wide range of studies. In this work, attention has been particularly focused on the study of Ru^{II} complexes.

The bonding properties of ruthenium complexes can be explained by crystal field theory and molecular orbital theory. From the point of view of crystal field theory, the properties of ruthenium complexes arise from electrostatic interactions between the metal ion and chelating ligands, which result in the splitting of d-orbital energies. From the point of view of molecular orbital theory, the properties of ruthenium can be explained by the charge transfer between the metal and chelating ligands as a result of the interactions between the s, p and d atomic orbitals of the metal centre that have an appropriate geometry to those of the chelating ligands.

The coordination chemistry of ruthenium with oligopyridine ligands has been extensively studied. As many polypyridyl ligands are available, ruthenium polypyridyl complexes are extremely versatile with wide-ranging photophysical, photochemical and redox properties, which can be optimised for a particular purpose.[76] In addition to the many well-known synthetic reactions for the preparation of ruthenium complexes, the possibility of functionalisation of these ligands with appropriate anchoring groups allows the attachment of these complexes onto a variety of surfaces.

Properties of Ruthenium Complexes with Polypyridyl Ligands

Photophysical and Photochemical Properties

A photochemical or photophysical process takes place when a molecule absorbs a photon and promotes an electron from the ground state to the excited state. This high-energy state is unstable, and, thus, the molecule tends to undergo some type of deactivation process. Excited-state deactivation can occur through (i) the emission of light (luminescence), (ii) the liberation of the excess energy in the form of heat (thermal deactivation), (iii) the interaction with other molecules present in the local environment (quenching process) and (iv) the formation of a new species (photochemical reaction).[77]

The photochemistry of ruthenium complexes coordinated to different polypyridyl ligands has been extensively investigated in the last few decades.[7] Specifically, the prototype molecule $[Ru(bpy)_3]^{2+}$ has been one of the most studied molecules because of its high stability, strong and long-lived luminescence and ability to undergo redox reactions.

Absorption Spectroscopy

Polypyridyl complexes of Ru^{II} have a d^6 electronic configuration and a preferred octahedral geometry. Surrounding the metal ion, polypyridine ligands interact with ruthenium through σ-donor orbitals located on the nitrogen atoms and π-donor and π*-acceptor molecular orbitals delocalised on the aromatic rings.[7] The spectroscopic and electrochemical properties of ruthenium complexes are usually described through a simplified linear combination of atomic orbitals (Figure 11).[78] Each molecular orbital is denominated as metal (M) or ligand (L) in agreement with its prevalent localisation.

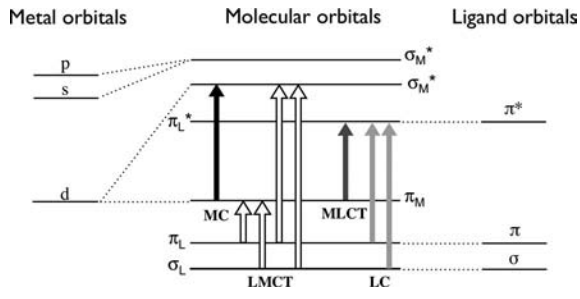

Figure 11. Simplified molecular orbital diagram showing different electronic transitions for a transition-metal complex in an octahedral geometry.

The molecular orbital diagram for an octahedral complex of a transition metal such as Ru^{II} indicates that different transitions between the different chelating ligand and metal orbitals can take place upon the absorption of light. These transitions can be classified as (i) metal-centred transitions (MC), also called d–d transitions, when the electrons are promoted from a π_M metal orbital to a σ^*_M orbital, (ii) ligand-centred (LC) or π–π^* ligand-to-ligand transitions, for transitions mainly localised on the chelating ligands and (iii) transitions between molecular orbitals with different localisation: metal-to-ligand charge transfer (MLCT), or ligand-to-metal charge transfer transitions (LMCT). Electronic transitions that occur to a lesser extent are those from a metal-centred orbital to solvent (charge transfer to solvent, CTTS) or between two orbitals mainly located on different chelating ligands (ligand-to-ligand charge transfer, LLCT).[78]

The light absorption processes are only allowed for transitions in which the ground and the excited state have the same spin value. These transitions can be observed as intense bands in the absorption spectra of the molecules. On the other hand, transitions from the ground state to excited states with different spin values are considered forbidden and can rarely be observed in absorption spectra.

The MC, MLCT and LC transitions of an octahedral transition-metal complex are related to the ligand field strength, the redox potential of the metal complex and the intrinsic properties of the ligands, respectively.[79] For this reason, changes in the molecular structure of the ligands attached to the ruthenium metal ion can dramatically vary the relative energy positions of the excited states, with the consequent change in their photophysical properties.[80]

Emission Spectroscopy

The behaviour of excited species is usually represented in a Jablonski diagram (Figure 12). In most ruthenium polypyridyl complexes, three states are involved in the photochemical activation process: a singlet ground state and a singlet and triplet excited state.

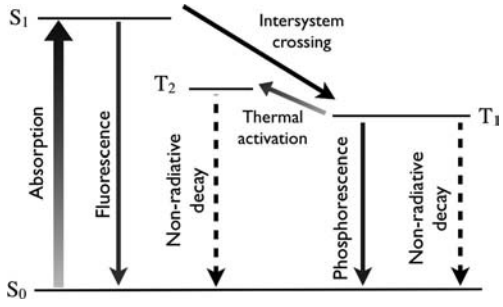

Figure 12. Jablonski diagram for ruthenium polypyridyl complexes.

The multiplicity of the ground state for most ruthenium (II) polypyridyl complexes is a singlet (S_0), and the absorption of a photon leads to promotion of an electron from an occupied orbital to a higher-energy unoccupied orbital with the same spin multiplicity (S_1). However, the lowest excited state is often a triplet (T_1) and, although it cannot be populated with excited electrons directly by light absorption, it can be through the deactivation of higher excited states. The S_1 state rapidly decays by intersystem crossing to T_1 because of strong spin–orbital coupling in metal complexes.[76a] The quantum yield for the formation of the lowest triplet excited state is often equal to 100%, which yields a short-lived fluorescence. Photo-excited state deactivation occurs though both a radiative (phosphorescence) and a non-radiative pathway.

Most ruthenium bipyridyl complexes show a lowest excited state as a triplet T_1, whose deactivation results in an intense long-lived luminescence. However, at high temperatures, radiationless deactivation can take place via a thermally activated T_2 metal-centred excited state.

The behaviour of ruthenium terpyridyl complexes is completely different from their bipyridyl analogues.[81] No emission is detected at room temperature in ruthenium terpyridyl complexes because of non-radiative relaxation of the excited state (T_1) by transition from a T_2 metal-centred excited state to the ground state. However, when the temperature decreases, the transition is less efficient and some luminescence can be observed. Furthermore, the optical properties of these complexes can be modified by introduction of substituents on the ligands, which allows improvement in the luminescence quantum efficiency and/or lifetime.[82]

The observed excited state lifetime (τ) of the ruthenium polypyridyl complexes depends on the rate constants for radiative (k_r) and non-radiative (k_{nr}) decays to the ground state. The term k_{nr} includes the non-radiative decays from the excited state T_1 and the thermally activated excited state T_2 to the ground state. The thermal population of the metal-centred T_2 state can be described by the Arrhenius equation: $k_t \cdot (e^{-E_a/RT})$ {where k_t is the prefactor for the thermally activated process and E_a is the activation energy barrier to the T_2 state [Equation (10)].[83] The relationship between the emission quantum yield (Φ) and k_r is given by [Equation (11)], (η_{isc}) is the efficiency of intersystem crossing, normally considered unity}.

$$1/\tau = k_r + k_{nr} \quad (10)$$

$$\Phi = \eta_{isc} \cdot k_r \cdot \tau \quad (11)$$

The thermal population of the short-lived metal-centred states has an important effect on the excited state lifetime of the molecules. Some ruthenium bis(tridentate) complexes show fast emission decays because of the non-radiative deactivation of the lowest excited state T_1 by thermal population of the metal-centred orbital T_2. For this reason, an increase in the energy gap between the T_1 and the T_2 excited states is a good approach for increasing the excited state lifetime.[84]

Redox Properties

Ru^{II} polypyridyl complexes are octahedral and diamagnetic, with a t_{2g}^6 configuration. However, because of their high number of stable oxidation states, ruthenium polypyri-

dyl complexes serve as both electron acceptors and electron donors.[85]

The oxidation of a d^6 Ru^{II} polypyridine complex involves removal of an electron from the HOMO, usually a π_M (t_{2g}) metal-centred orbital, with the formation of paramagnetic low-spin d^5 Ru^{III} complexes, which are inert to ligand substitution [Equation (12)].

$$[Ru^{II}(NN)_3]^{2+} \rightarrow [Ru^{II}(NN)_3]^{3+} + e^- \quad (12)$$

On the other hand, the reduction of a Ru^{II} polypyridyl complex may involve the introduction of one electron into the lowest-unoccupied molecular orbital, either into a metal-centred (σ^*_M) or a ligand-centred orbital (π^*_L), depending on their relative energy level arrangement. Generally, polypyridine ligands coordinated to ruthenium metal ions are easily reduced, and the reduction takes place on the ligand [Equation (13)]. In this case, ruthenium metal ions maintain their d^6 low-spin configuration. These species are usually inert, and the reduction reaction is reversible. However, when the lowest-energy empty orbital is a metal-centred orbital, the electron is added to the metal-centred orbital. The reduction of these complexes produces an unstable low-spin d^7 electronic configuration, which leads to a rapid ligand dissociation; this makes the reaction irreversible [Equation (14)].

$$[Ru^{II}(NN)_3]^{2+} + e^- \rightarrow [Ru^{II}(NN)_2(NN^{-})]^{2+} \quad (13)$$

$$[Ru^{II}(NN)_3]^{2+} + e^- \rightarrow [Ru^{I}(NN)_3]^{+} \rightarrow [Ru^{I}(NN)_2]^{+} + NN \quad (14)$$

The electrochemical behaviour of polypyridyl ruthenium complexes depends on the nature of the ligands surrounding the metal ion. The redox potentials of a metal couple can be predicted by using the ligand electrochemical parameters (E_L) described by Lever in 1990.[86] E_L is a function of the σ- and π-donor and -acceptor properties of the ligand and is independent of the metal to which the ligand is bound.[87]

Tuning of Spectro- and Electrochemical Properties

The structure of the polypyridyl ligand determines the redox and spectroscopic properties of the ruthenium complex, which can be modified by introduction of appropriate chelating ligands.[29b] Generally, two strategies are used to tune these properties: (i) the modification of the LUMO energy level by introducing a ligand with a low-lying π* molecular orbital involved in the MLCT or (ii) by destabilisation of the t_{2g} metal orbital (HOMO energy level), which is affected by the donor- or acceptor properties of the ligands (Figure 13).[88]

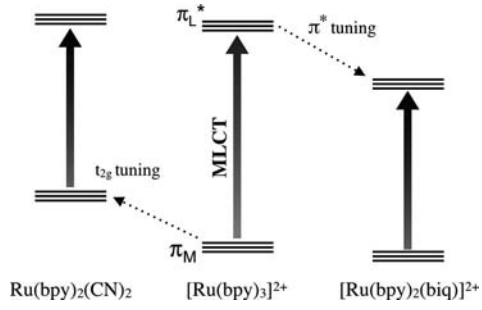

Figure 13. Tuning of HOMO (t_{2g}) and LUMO (π*) orbital energy in various ruthenium polypyridyl complexes.

The modification of the HOMO and LUMO energy levels has a direct effect over the MLCT transitions of the ruthenium complexes, and, consequently, induces a change in the absorption spectra of the molecule. Controllable adjustments of the excited-state energy levels can be performed with an appropriate selection of the ligands involved in the MLCT (e.g. $[Ru(bpy)_3]^{2+}$ and $[Ru(bpy)_2(biq)]^{2+}$, where (bpy) is 2,2′-bipyridine and biq 2,2′-biquinoline). However, smaller changes in the LUMO energy levels are induced by the simple introduction of substituents on the aromatic rings of the ligands (e.g. $[Ru(bpy)_3]^{2+}$ and $[Ru(4,4'\text{-dimethyl-}2,2'\text{-bipyridine})_3]^{2+}$). Furthermore, considerable changes in the spectral properties of the ruthenium complexes can be achieved upon substitution of a ligand not involved in the MLCT transition by a nonchromophoric donor ligand, which destabilises the metal t_{2g} orbitals (e.g. $[Ru(bpy)(biq)_2]^{2+}$ and $[Ru(biq)_2(CN)_2]$).

Stereochemistry of Ruthenium Polypyridyl Complexes

Another characteristic of octahedral metal complexes such as Ru^{II} with bidentate ligands is their stereoisomerism.[89] For homoleptic tris(bidentate) complexes with symmetrical ligands (NN), two enantiomers are possible, Δ and Λ (Figure 14a). Two geometrical isomers [facial (*fac*) and

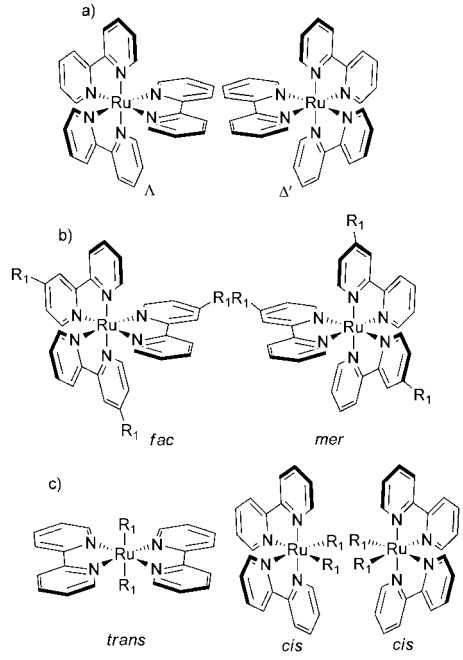

Figure 14. (a) Λ and Δ geometrical isomers of Ru^{II} symmetrical tris(bidentate) complexes, (b) *fac* and *mer* isomers of Ru^{II} tris(bidentate) complexes containing unsymmetrical ligands, and (c) *trans* and two *cis* isomers of bis(bidentate) ruthenium complexes. (R_1 corresponds to substituents).

meridional (*mer*)] are possible for complexes with nonsymmetrical bidentate chelate ligands (R-NN) (Figure 14b). However, the number of isomers increases to four and eight, respectively, when two $[Ru(R_1\text{-}NN_1)(R_2\text{-}NN_2)(NN)]$ or three $[Ru(R_1\text{-}NN_1)(R_2\text{-}NN_2)(R_3\text{-}NN_3)]$ unsymmetrical substituted ligands are linked to the ruthenium metal centre (R_1-NN_1, R_2-NN_2 and R_3-NN_3 are different unsymmetrical nitrogen-containing bidentate chelate ligands). For bis(bidentate) complexes two geometrical isomers can be formed (*cis*/*trans*) as well as two enantiomers of the *cis* form (Figure 14c). Furthermore, the number of possible isomers increases exponentially with the number of metal ions in the synthesis of polynuclear complexes.

In order to avoid stereochemical problems, several approaches have been used in the enantioselective synthesis of ruthenium complexes, such as the use of tridentate instead of bidentate ligands,[90] the utilisation of chiral building blocks to synthesise complexes with a predetermined stereochemistry[91] and the light-induced isomerism in ruthenium complexes.[92]

The stereochemical problems are solved when tridentate ligands such as terpyridine (tpy) are used, which are coordinated to the ruthenium metal centre in a meridional form to create an achiral centre. Furthermore, the introduction of a substituent in the 4′-position of the terpyridine does not increase the number of geometrical isomers (Figure 15).

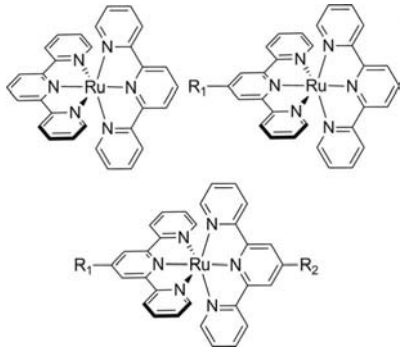

Figure 15. Ruthenium tris(bidentate) polypyridyl complexes without (top left), with one (top right), and with two (bottom) substituents in the 4′-position. (R_1 and R_2 correspond to different substituents).

Synthesis of Ruthenium Polypyridyl Complexes

Ruthenium polypyridyl complexes have an extensive and well-known synthetic chemistry.[93] Their compounds show high stability and flexibility with a wide range of mono-, bi-, tri- and tetradentate ligands. Furthermore, ligands can be exchanged sequentially, by removing some of them while maintaining the presence of others as well as the stereochemical integrity.

One of the most common synthetic precursor for ruthenium mononuclear polypyridyl complexes is the commercially available $RuCl_3{\cdot}xH_2O$. Some important intermediates in the synthesis of homo- and heteroleptic complexes such as $[Ru(CO)_2Cl_2]_n$,[94] $[Ru(DMSO)_4Cl_2]$[95] (DMSO = dimethylsulfoxide), $[Ru(\eta^6\text{-arene})Cl_2]_2$,[96] $[Ru(COD)Cl_2]_n$[97] (COD = 1,5-cyclooctadiene) can be synthesised in one step from $RuCl_3{\cdot}xH_2O$. Several synthetic routes for the synthesis of homoleptic and heteroleptic polypyridyl ruthenium complexes are detailed below.

Synthesis of Tris(bidentate) Ruthenium Complexes

The first synthesis of an homoleptic ruthenium compound reported in 1936 corresponds to the complex $[Ru(bpy)_3]Cl_2$.[98] The heating at reflux of $RuCl_3{\cdot}xH_2O$ with an excess of a bipyridyl compound (NN) results in the formation of ruthenium homoleptic tris(bidentate) ligand. This synthesis was extended to the incorporation of a wide range of bidentate ligands with the addition of a reducing agent such as phosphinic acid or hydroxylamine hydrochloride to the reaction mixture.[99]

Although the most simple reaction to obtain ruthenium tris(bipyridyl) complexes is based on ruthenium(III) trichloride, homoleptic compounds can also be prepared from other precursors such as $[Ru(\eta^6\text{-arene})Cl_2]_2$,[96] $[Ru(CO)_2Cl_2]_n$,[100] $[Ru(DMSO)_4Cl_2]$[101] or $[Ru(COD)Cl_2]_n$,[102] which involve a two-step reaction (Figure 16).

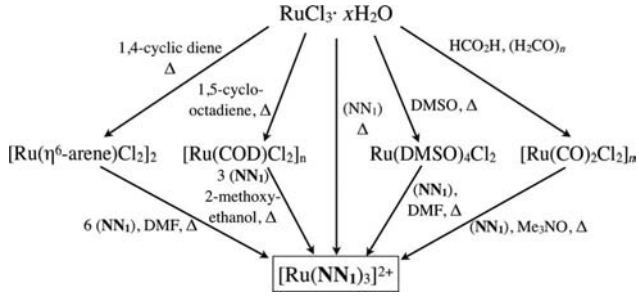

Figure 16. Synthetic routes of homoleptic ruthenium complexes containing three bidentate ligands. (NN_1) is a bidentate chelate ligand.

An interesting alternative to previous synthetic routes, which offers a reduction in the reaction time, consists of the microwave-assisted reaction of different precursors such as $RuCl_3{\cdot}xH_2O$[103] or $[Ru(p\text{-cymene})Cl_2]_2$.[104]

Synthesis of Ruthenium Bis-Heteroleptic Complexes

In some cases, the coordination of different chelate ligands to the metal ion is necessary in order to modify the spectroscopic and electrochemical properties of the ruthenium complex for a specific application. Synthetic routes for ruthenium complexes of the type $[Ru(NN_1)_2(NN_2)]^{2+}$ are based on the sequential introduction of ligands to a ruthenium precursor.

A widely used synthetic approach involves the introduction of two chelate ligands by direct reaction of $RuCl_3{\cdot}xH_2O$ with two equivalents of the bidentate ligand, to obtain a $[Ru(NN_1)_2Cl_2]$ complex. Other precursors used in the synthesis of such complexes are $Ru(COD)Cl_2$[105] and $Ru(DMSO)_4Cl_2$,[106] with the disadvantage of involving more than one synthetic step. Subsequent introduction of a

third diimine to the $[Ru(NN_1)_2Cl_2]$ complex in an appropriate medium results in the formation of $[Ru(NN_1)_2(NN_2)]^{2+}$ (Figure 17).[107]

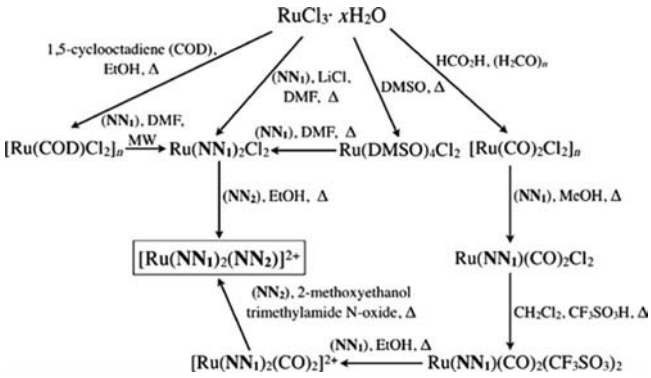

Figure 17. Synthetic routes for bis-heteroleptic ruthenium complexes containing three bidentate ligands. The (NN_1) and (NN_2) are different bidentate chelate ligands.

Another synthetic method to obtain ruthenium bis-homoleptic complexes is based on the sequential introduction of three chelate ligands to the $[Ru(CO)_2Cl_2]_n$ oligomer.[108]

Synthesis of Ruthenium Tris-Heteroleptic Complexes

Several synthetic methodologies have been developed for the preparation of ruthenium tris-heteroleptic complexes. All of these synthetic routes are based on the sequential introduction of chelate ligands by substitution of labile ligands.

Two synthetic routes for the synthesis of $[Ru(NN_1)(NN_2)(NN_3)]^{2+}$ complexes with $[Ru(CO)_2Cl_2]_n$ as a starting material have been extensively studied (Figure 18). The first step in both methodologies is the introduction of one chelate ligand. The subsequent decarbonylation step differs. In the first method, the labile CO ligands are substituted by the application of heat,[109] while in the second, decarbonylation takes place by irradiation with UV light.[110]

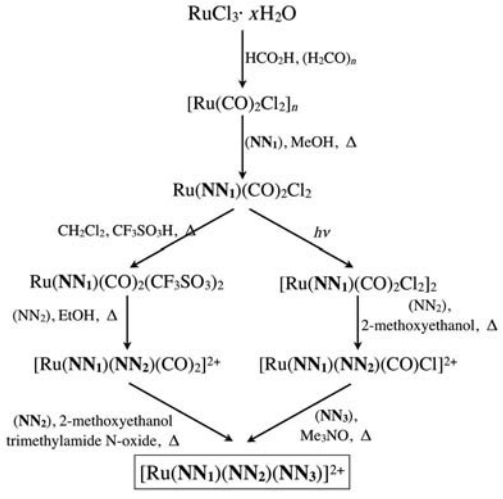

Figure 18. Synthetic routes for tris-heteroleptic ruthenium complexes containing three bidentate ligands by using carbonyl complexes as a precursor. (NN_1), (NN_2) and (NN_3) are different bidentate chelate ligands.

Other widely studied synthetic routes are based on synthesising $Ru(NN_1)(NN_2)Cl_2$ intermediates, by using different precursors such as $RuCl_3{\cdot}xH_2O$,[107] $Ru(DMSO)_4Cl_2$[111] or $[Ru(\eta^6\text{-arene})Cl_2]_2$[96] as starting materials and subsequent sequential introduction of chelate ligands under different reaction conditions (Figure 19).

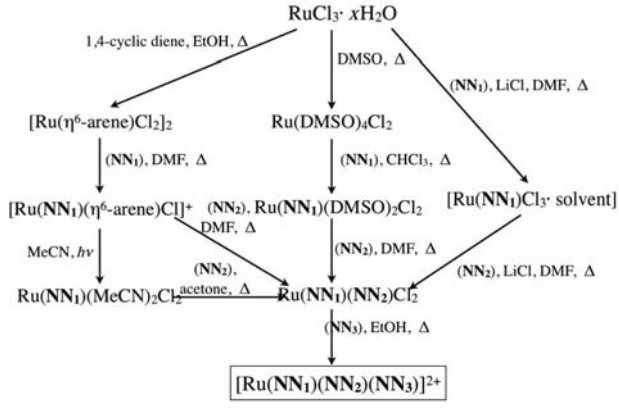

Figure 19. Synthetic routes for tris-heteroleptic ruthenium complexes containing three bidentate ligands by using different precursors. (NN_1), (NN_2) and (NN_3) are different bidentate chelate ligands.

Synthesis of Bis(tridentate) Ruthenium Complexes

Complexation of ruthenium metal ions with two tridentate ligands leads to the formation of a complex with a distorted octahedral geometry.[112] Synthetic routes involve a two-step sequence, with the successive introduction of two equal or different tridentate ligands.

The most widely used synthetic method uses $RuCl_3{\cdot}3H_2O$ as a precursor. The introduction of the first ligand results in the formation of $Ru(NNN_1)Cl_3$, where (NNN) is a nitrogen-containing tridentate ligand. A reducing agent for the $Ru^{III} \rightarrow Ru^{II}$ conversion is necessary when the second ligand is coordinated to the metal ion.[82] This synthetic approach allows the synthesis of both homoleptic and heteroleptic ruthenium complexes by applying the same ligand twice or two different ligands. Furthermore, this synthesis can be carried out within a microwave, which saves an enormous amount of time (Figure 20).[113]

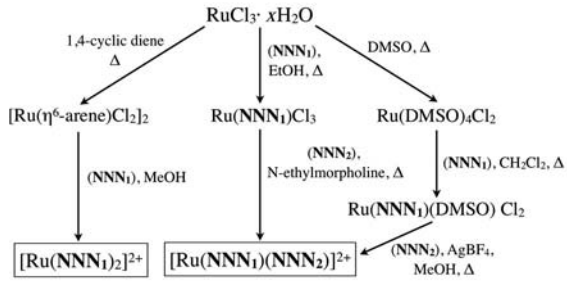

Figure 20. Synthetic routes for tris-heteroleptic ruthenium complexes containing two tridentate ligands by using different precursors. (NNN_1) and (NNN_2) are different tridentate chelate ligands.

An alternative procedure for ligands that can easily decompose is the synthesis under mild conditions of bis(tridentate) ruthenium complexes with $Ru(DMSO)_4Cl_2$ as a starting material.[114]

A third synthetic strategy is available for obtaining symmetric bis(tridentate) complexes by reacting $[Ru(\eta^6\text{-arene})Cl_2]_2$ with two equivalents of the ligand.[115]

Relationship between Dye Molecular Structure and DSSC Performance

As mentioned before, the molecular structure of the dye affects not only their absorption, photophysical and redox properties, but also the electron-transfer processes occurring at the TiO_2/dye/electrolyte surface.[116] These parameters strongly determine the overall efficiency of the device.

The use of photosensitisers such as Ru^{II} polypyridyl complexes with low molar extinction coefficients requires DSSC devices with thicker TiO_2 films in order to have enough dye present to capture as many of the incident photons as possible. However, this results in a decreased V_{oc} because of an increase in the surface area, which provides additional e^--TiO_2/electrolyte$^+$ recombination sites.[117] For this reason, some developments in the design of new ruthenium polypyridyl photosensitisers have arisen from the enhancement of the optical absorption. One of the best routes to improve the light-harvesting capability of ruthenium complexes is through the extension of the pyridyl ligands with the introduction of π-conjugated donor- or acceptor systems (Figure 21).

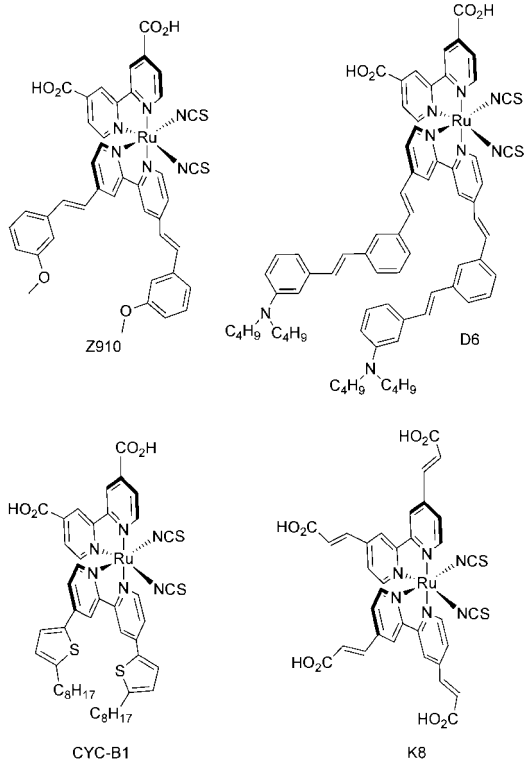

Figure 21. Molecular structure of highly π-conjugated ruthenium polypyridyl complexes.

Ideally, the photosensitiser absorption spectrum should overlap as much as possible with that of the solar spectrum. Sequential tuning of the HOMO and LUMO energy levels through the incorporation of strong σ-electron donor or low-lying π* groups can be performed in order to extend the absorption spectrum of the dye to the near IR region.[80] These modifications involve a decrease in the HOMO–LUMO gap, but the position of the HOMO and LUMO energy levels of the dye have to be such as to maintain sufficient driving force to allow both efficient electron injection into TiO_2 and dye regeneration by the iodide/triiodide redox couple.

One of the most commonly used approaches to produce a redshift in the absorption spectra of Ru^{II} polypyridyl complexes is through destabilisation of the HOMO energy level with the introduction of electron-donor ligands. Most ruthenium polypyridyl complexes used in DSSCs contain thiocyanate ancillary ligands to shift the absorption spectra towards longer wavelengths.[118] However, NCS ligands are believed to be the weakest moiety of this type of complexes when exposed to light or high temperatures.[119] The replacement of the thiocyanate moieties by chelates, such as cyclometalated bi- and tridentate ligands, can lead to the preparation of more stable chromophores (Figure 22).[120]

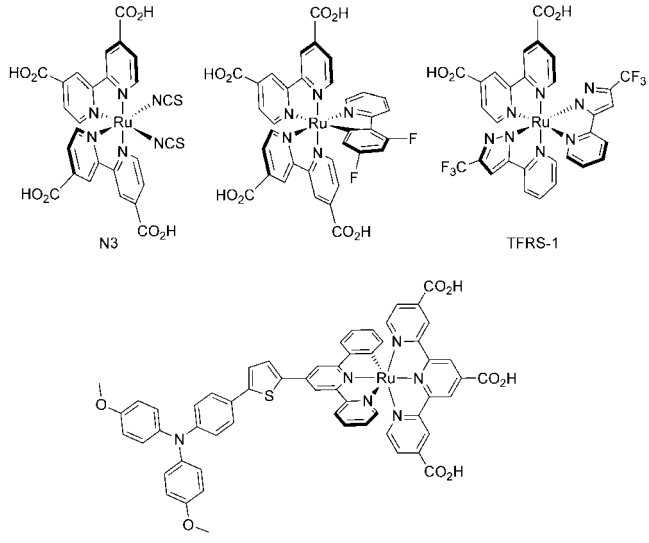

Figure 22. Molecular structure of ruthenium polypyridyl complexes with a bathochromic shift in the absorption spectra as a result of the presence of σ-donor ancillary ligands.

Another way to decrease the HOMO–LUMO gap has been achieved with the introduction of ligands containing low-lying π* orbitals, such as highly conjugated polypyridyl ligands (Figure 23).[121]

An important issue for molecular photovoltaics is to achieve fast and efficient electron injection into the metal oxide. This can be obtained by a strong attachment of the dye onto the surface of the semiconductor, as well as by a sufficiently high LUMO energy level of the photosensitiser. In addition, the LUMO energy level should be located in the ligands containing the groups anchored onto the TiO_2 surface, in order to obtain an effective coupling between the

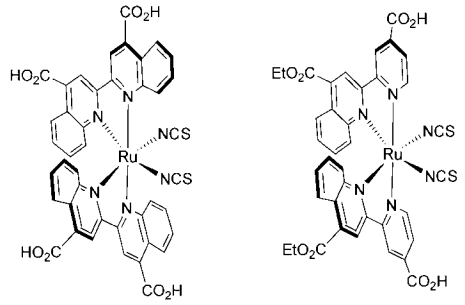

Figure 23. Molecular structure of ruthenium complexes containing ligands with low-lying π* molecular orbitals.

dye and the metal oxide orbitals. Covalent bonds between the anchoring groups of the ruthenium polypyridyl complex and the hydroxy groups present on the surface of the TiO_2 nanoparticles allow for strong electron coupling between the photosensitiser and the semiconductor.[18] Different anchoring groups have been tested, but the most common anchoring group in ruthenium complexes are carboxylic acids (Figure 24). Carboxylic acid groups can easily be hydrolysed in the presence of water or basic media, which results in dye desorption from the TiO_2 surface. A strategy to prevent the hydrolysation of the link between the dye and TiO_2 is the substitution of carboxylic acid groups by more stable linkers such as phosphonic acid.[19,122]

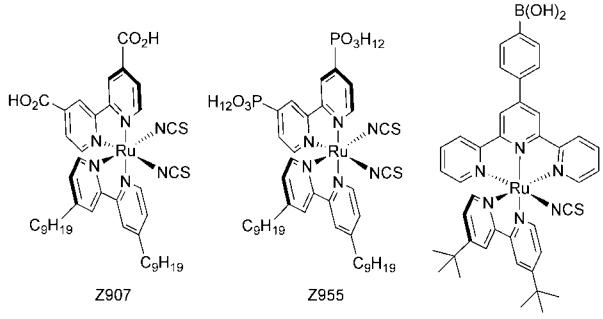

Figure 24. Molecular structure of ruthenium polypyridyl complexes containing different anchoring groups.

Furthermore, dyes attached to the surface of the metal oxide can be desorbed by the presence of water in the electrolyte, which is obviously a concern for the long-term stability of DSSCs.[123] The incorporation of hydrophobic alkyl chains to the pyridyl ligand can decrease dye desorption and increase cell stability by preventing the accumulation of water molecules near the TiO_2 surface (Figure 25).[29a,124]

The spatial separation between the oxidised dye and the semiconductor surface has an important effect on the charge-recombination dynamics between the sensitiser and the electrons at TiO_2.[24a] Increasing this distance and minimising recombination can be achieved by the attachment of electron-donor groups[125] or rigid spacers[126] to the polypyridyl ligands that are able to locate the cationic charges at long distances from the TiO_2 surface (Figure 26).

The recombination reaction between the photoinjected electrons and the oxidised electrolyte strongly affects the

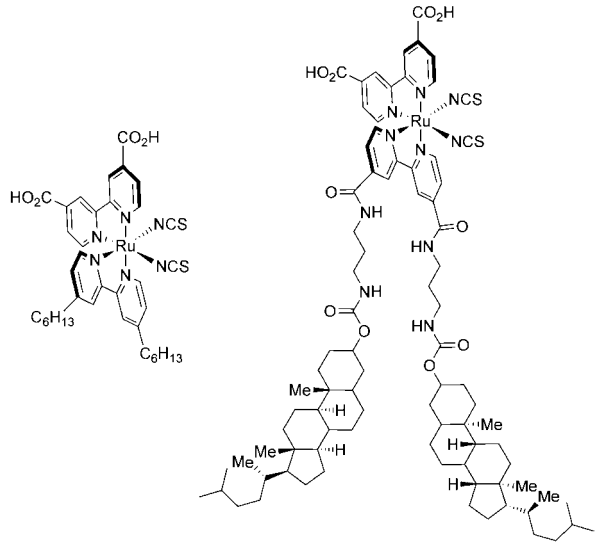

Figure 25. Molecular structure of two amphiphilic ruthenium polypyridyl complexes.

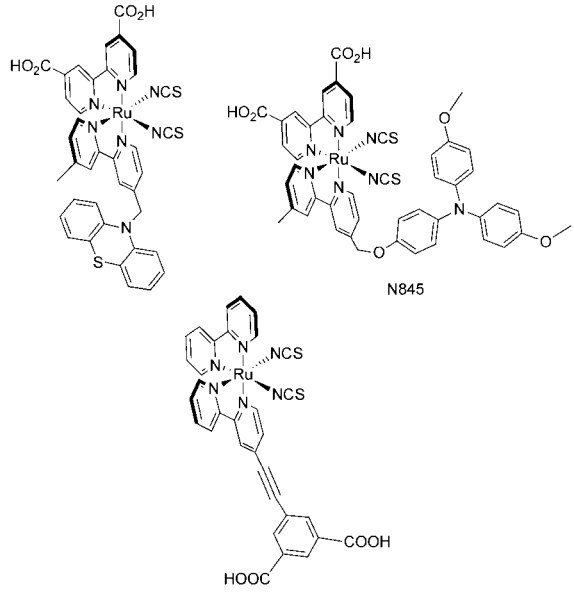

Figure 26. Ruthenium polypyridyl complexes that increase the distance between the dye cation and the TiO_2 surface by the introduction of electron-donor groups or rigid spacers into the dye structure.

V_{oc} of the device and, thus, the final overall efficiency. The incorporation of long alkyl chains and the degree of protonation of the ruthenium photosensitisers are key factors in the reduction of the e^--TiO_2/electrolyte$^+$ recombination reaction. Amphiphilic dyes can block the approach of the oxidised electrolyte to the semiconductor surface, while control of the degree of protonation of the acid anchoring groups prevents the downward shift of the semiconductor conduction band edge caused by surface protonation. The protons of ruthenium polypyridyl sensitisers can be substituted by tetrabutylammonium cations (TBA), sodium cations or other counterions (Figure 27).[127]

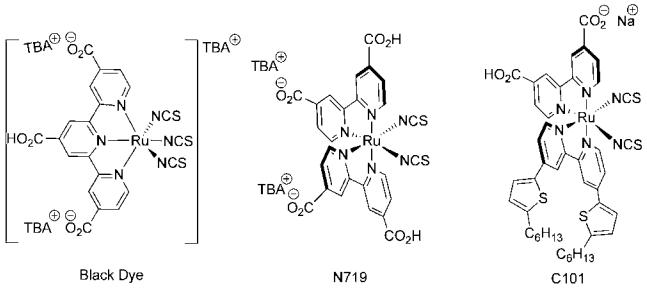

Figure 27. Ruthenium polypyridyl complexes with various counterions.

Over the last years, our group, among others, have observed that the presence of certain atoms such as sulfur and oxygen[128] or chemical moieties[129] such as amino (-NH_2) or nitro (-NO_2) groups can have a dramatic influence over the device output efficiency (Figure 28). Indeed, the presence of certain chemical groups or atoms leads to faster electron-recombination dynamics, which affects the V_{oc} of the device. This observation is similar to the measured effects of the presence of highly conjugated molecular structures in organic sensitisers,[38a,130] and, thus, indicates that the dye molecular structure is directly involved in preventing or accelerating the interfacial charge-transfer reaction between the photoinjected electrons and the oxidised species present in the iodine/iodide electrolyte.

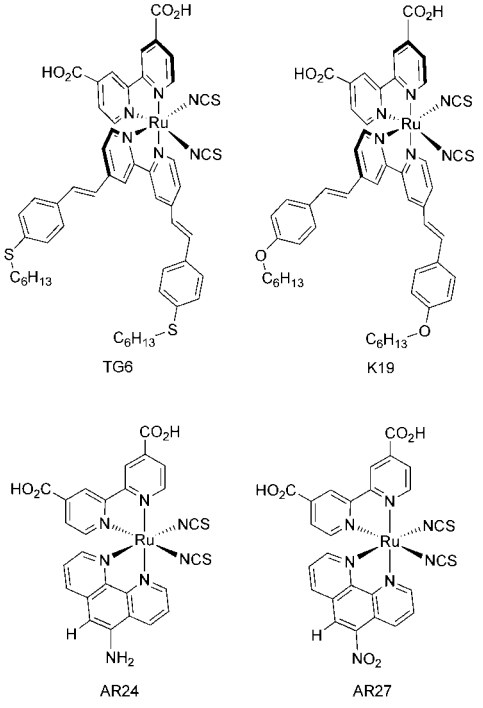

Figure 28. Ruthenium polypyridyl complexes with different ligand substituents.

Conclusions and Perspectives

The research of dye-sensitised solar cells is a growing research field. Novel sensitisers based on ruthenium polypyridyl complexes are published monthly, and a new generation of organic dyes are challenging, not only the light-to-energy conversion efficiencies of the former ruthenium dyes, but also their stability under working conditions. Indeed, the future looks bright for this incipient solar technology. However, many questions still need to be fully addressed. A deeper understanding of the role that the dye molecular structure plays over interfacial charge-transfer processes, both recombination or regeneration reactions, is a must. The discovery of novel electrolytes to avoid the use of iodine/iodide and to achieve higher open circuit voltages will be the next challenge for this research field. Promising results on "revisited" cobalt-based electrolytes open a new window to push further the efficiency and will certainly expand even more the interest in this new generation of solar cells. Finally, the long-standing proposed use of IR quantum dots that undergo multiple exciton generation under light irradiation should be also considered as a future research pathway towards the new generation of high efficiency solar cells.

Acknowledgments

We would like to thank the ICIQ, ICREA and the Spanish MICINN project CTQ2010-18859 for financial support and the Catalan Government for the 2009SGR207 grant. E. P. also thanks the EU for the ERCstg Polydot.

[1] *International Energy Outlook*, (US Dept of Energy, Washington DC), Energy Information Administration, **2010**.
[2] A. Ç. Köne, T. Büke, *Renewable Sustainable Energy Rev.* **2010**, *14*, 2906.
[3] N. S. Lewis, D. G. Nocera, *Proc. Natl. Acad. Sci. USA* **2006**, *103*, 15729.
[4] M. A. Green, *Phys. E* **2002**, *14*, 11.
[5] B. O'Regan, M. Grätzel, *Nature* **1991**, *353*, 737.
[6] G. J. Meyer, *ACS Nano* **2010**, *4*, 4337.
[7] S. Campagna, F. Puntoriero, F. Nastasi, G. Bergamini, V. Balzani, *Top. Curr. Chem.* **2007**, *280*, 117.
[8] A. Hagfeldt, G. Boschloo, L. Sun, L. Kloo, H. Pettersson, *Chem. Rev.* **2010**, *110*, 6595.
[9] S. M. Feldt, E. A. Gibson, E. Gabrielsson, L. Sun, G. Boschloo, A. Hagfeldt, *J. Am. Chem. Soc.* **2010**, *132*, 16714.
[10] A. B. F. Martinson, T. W. Hamann, M. J. Pellin, J. T. Hupp, *Chem. Eur. J.* **2008**, *14*, 4458.
[11] S. Hore, E. Palomares, H. Smit, N. J. Bakker, P. Comte, P. Liska, K. R. Thampi, J. M. Kroon, A. Hinsch, J. R. Durrant, *J. Mater. Chem.* **2005**, *15*, 412.
[12] a) C. J. Barbé, F. Arendse, P. Comte, M. Jirousek, F. Lenzmann, V. Shklover, M. Grätzel, *J. Am. Ceram. Soc.* **1997**, *80*, 3157; b) Q. Zhang, G. Cao, *Nano Today* **2011**, *6*, 91.
[13] M. Grätzel, *Inorg. Chem.* **2005**, *44*, 6841.
[14] K. D. Benkstein, N. Kopidakis, J. van de Lagemaat, A. J. Frank, *J. Phys. Chem. B* **2003**, *107*, 7759.
[15] N. Robertson, *Angew. Chem. Int. Ed.* **2006**, *45*, 2338.
[16] AM1.5G Global Solar Spectrum (ASTM G173–03) source of data ASTM/NREL, http://rredc.nrel.gov/solar/spectra/am1.5/.
[17] K. Kalyanasundaram, M. Grätzel, *Coord. Chem. Rev.* **1998**, *177*, 347.
[18] E. Galoppini, *Coord. Chem. Rev.* **2004**, *248*, 1283.
[19] I. Gillaizeau-Gauthier, F. Odobel, M. Alebbi, R. Argazzi, E. Costa, C. A. Bignozzi, P. Qu, G. J. Meyer, *Inorg. Chem.* **2001**, *40*, 6073.

[20] S. Altobello, C. A. Bignozzi, S. Caramori, G. Larramona, S. Quici, G. Marzanni, R. Lakhmiri, *J. Photochem. Photobiol. A: Chem.* **2004**, *166*, 91.
[21] P. Ghosh, T. G. Spiro, *J. Am. Chem. Soc.* **1980**, *102*, 5543.
[22] A. Kathiravan, R. Renganathan, *J. Colloid Interface Sci.* **2009**, *331*, 401.
[23] a) A. Vittadini, A. Selloni, F. P. Rotzinger, M. Gratzel, *J. Phys. Chem. B* **2000**, *104*, 1300; b) T. J. Meyer, G. J. Meyer, B. W. Pfennig, J. R. Schoonover, C. J. Timpson, J. F. Wall, C. Kobusch, X. Chen, B. M. Peek, *Inorg. Chem.* **1994**, *33*, 3952.
[24] a) J. N. Clifford, E. Palomares, M. K. Nazeeruddin, M. Grätzel, J. Nelson, X. Li, N. J. Long, J. R. Durrant, *J. Am. Chem. Soc.* **2004**, *126*, 5225; b) S. A. Haque, S. Handa, K. Peter, E. Palomares, M. Thelakkat, J. R. Durrant, *Angew. Chem. Int. Ed.* **2005**, *44*, 5740.
[25] A. S. Polo, M. K. Itokazu, N. Y. Murakami Iha, *Coord. Chem. Rev.* **2004**, *248*, 1343.
[26] a) A. Mishra, M. K. R. Fischer, P. Bäuerle, *Angew. Chem. Int. Ed.* **2009**, *48*, 2474; b) Y. Ooyama, Y. Harima, *Eur. J. Org. Chem.* **2009**, 2903.
[27] G. P. Smestad, M. Gratzel, *J. Chem. Educ.* **1998**, *75*, 752.
[28] C. A. Bignozzi, R. Argazzi, C. J. Kleverlaan, *Chem. Soc. Rev.* **2000**, *29*, 87.
[29] a) M. K. Nazeeruddin, S. M. Zakeeruddin, J. J. Lagref, P. Liska, P. Comte, C. Barolo, G. Viscardi, K. Schenk, M. Grätzel, *Coord. Chem. Rev.* **2004**, *248*, 1317; b) A. Islam, H. Sugihara, H. Arakawa, *J. Photochem. Photobiol. A: Chem.* **2003**, *158*, 131.
[30] a) T. A. Heimer, C. A. Bignozzi, G. J. Meyer, *J. Phys. Chem.* **1993**, *97*, 11987; b) D. Kuciauskas, M. S. Freund, H. B. Gray, J. R. Winkler, N. S. Lewis, *J. Phys. Chem. B* **2001**, *105*, 392; c) S. Altobello, R. Argazzi, S. Caramori, C. Contado, S. Da Fre, P. Rubino, C. Chone, G. Larramona, C. A. Bignozzi, *J. Am. Chem. Soc.* **2005**, *127*, 15342.
[31] a) A. Islam, H. Sugihara, K. Hara, L. P. Singh, R. Katoh, M. Yanagida, Y. Takahashi, S. Murata, H. Arakawa, G. Fujihashi, *Inorg. Chem.* **2001**, *40*, 5371; b) E. A. M. Geary, L. J. Yellowlees, L. A. Jack, I. D. H. Oswald, S. Parsons, N. Hirata, J. R. Durrant, N. Robertson, *Inorg. Chem.* **2005**, *44*, 242.
[32] G. M. Hasselmann, G. J. Meyer, *J. Phys. Chem. B* **1999**, *103*, 7671.
[33] a) N. Alonso-Vante, J.-F. Nierengarten, J.-P. Sauvage, *J. Chem. Soc., Dalton Trans.* **1994**, 1649; b) T. Bessho, E. C. Constable, M. Grätzel, A. H. Redondo, C. E. Housecroft, W. Kylberg, M. K. Nazeeruddin, M. Neuburger, S. Schaffner, *Chem. Commun.* **2008**, 3717.
[34] a) S. Ferrere, *Chem. Mater.* **2000**, *12*, 1083; b) S. Ferrere, B. A. Gregg, *J. Am. Chem. Soc.* **1998**, *120*, 843.
[35] M. K. Nazeeruddin, F. De Angelis, S. Fantacci, A. Selloni, G. Viscardi, P. Liska, S. Ito, B. Takeru, M. Grätzel, *J. Am. Chem. Soc.* **2005**, *127*, 16835.
[36] R. Argazzi, G. Larramona, C. Contado, C. A. Bignozzi, *J. Photochem. Photobiol. A: Chem.* **2004**, *164*, 15.
[37] a) H. Imahori, T. Umeyama, S. Ito, *Acc. Chem. Res.* **2009**, *42*, 1809; b) M. V. Martinez-Diaz, G. de la Torre, T. Torres, *Chem. Commun.* **2010**, *46*, 7090.
[38] a) W. Zeng, Y. Cao, Y. Bai, Y. Wang, Y. Shi, M. Zhang, F. Wang, C. Pan, P. Wang, *Chem. Mater.* **2010**, *22*, 1915; b) T. Bessho, S. M. Zakeeruddin, C.-Y. Yeh, E. W.-G. Diau, M. Grätzel, *Angew. Chem. Int. Ed.* **2010**, *49*, 6646.
[39] D. P. Hagberg, J.-H. Yum, H. Lee, F. De Angelis, T. Marinado, K. M. Karlsson, R. Humphry-Baker, L. Sun, A. Hagfeldt, M. Grätzel, M. K. Nazeeruddin, *J. Am. Chem. Soc.* **2008**, *130*, 6259.
[40] Z.-S. Wang, Y. Cui, Y. Dan-oh, C. Kasada, A. Shinpo, K. Hara, *J. Phys. Chem. C* **2007**, *111*, 7224.
[41] J.-H. Yum, P. Walter, S. Huber, D. Rentsch, T. Geiger, F. Nüesch, F. De Angelis, M. Grätzel, M. K. Nazeeruddin, *J. Am. Chem. Soc.* **2007**, *129*, 10320.
[42] T. Edvinsson, C. Li, N. Pschirer, J. Schöneboom, F. Eickemeyer, R. Sens, G. Boschloo, A. Herrmann, K. Müllen, A. Hagfeldt, *J. Phys. Chem. C* **2007**, *111*, 15137.
[43] A. Forneli, M. Planells, M. A. Sarmentero, E. Martinez-Ferrero, B. C. O'Regan, P. Ballester, E. Palomares, *J. Mater. Chem.* **2008**, *18*, 1652.
[44] J. J. Cid, J. H. Yum, S. R. Jang, M. K. Nazeeruddin, E. Martinez-Ferrero, E. Palomares, J. Ko, M. Grätzel, T. Torres, *Angew. Chem. Int. Ed.* **2007**, *46*, 8358.
[45] F. G. Gao, A. J. Bard, L. D. Kispert, *J. Photochem. Photobiol. A: Chem.* **2000**, *130*, 49.
[46] A. Kay, M. Grätzel, *J. Phys. Chem.* **1993**, *97*, 6272.
[47] S. Tatay, S. A. Haque, B. O'Regan, J. R. Durrant, W. J. H. Verhees, J. M. Kroon, A. Vidal-Ferran, P. Gavina, E. Palomares, *J. Mater. Chem.* **2007**, *17*, 3037.
[48] F. T. Kong, S. Y. Dai, K. J. Wang, *Adv. OptoElec.* **2007**, 75384.
[49] a) Z.-S. Wang, K. Sayama, H. Sugihara, *J. Phys. Chem. B* **2005**, *109*, 22449; b) C. Teng, X. Yang, S. Li, M. Cheng, A. Hagfeldt, L.-z. Wu, L. Sun, *Chem. Eur. J.* **2010**, *16*, 13127.
[50] a) G. Oskam, B. V. Bergeron, G. J. Meyer, P. C. Searson, *J. Phys. Chem. B* **2001**, *105*, 6867; b) B. V. Bergeron, A. Marton, G. Oskam, G. J. Meyer, *J. Phys. Chem. B* **2004**, *109*, 937.
[51] P. Wang, S. M. Zakeeruddin, J.-E. Moser, R. Humphry-Baker, M. Grätzel, *J. Am. Chem. Soc.* **2004**, *126*, 7164.
[52] a) B. A. Gregg, F. Pichot, S. Ferrere, C. L. Fields, *J. Phys. Chem. B* **2001**, *105*, 1422; b) T. Daeneke, T.-H. Kwon, A. B. Holmes, N. W. Duffy, U. Bach, L. Spiccia, *Nat. Chem.* **2011**, *3*, 213.
[53] S. A. Sapp, C. M. Elliott, C. Contado, S. Caramori, C. A. Bignozzi, *J. Am. Chem. Soc.* **2002**, *124*, 11215.
[54] S. Hattori, Y. Wada, S. Yanagida, S. Fukuzumi, *J. Am. Chem. Soc.* **2005**, *127*, 9648.
[55] T. C. Li, A. M. Spokoyny, C. She, O. K. Farha, C. A. Mirkin, T. J. Marks, J. T. Hupp, *J. Am. Chem. Soc.* **2010**, *132*, 4580.
[56] H. Tian, X. Jiang, Z. Yu, L. Kloo, A. Hagfeldt, L. Sun, *Angew. Chem. Int. Ed.* **2010**, *49*, 7328.
[57] N. Kopidakis, E. A. Schiff, N. G. Park, J. van de Lagemaat, A. J. Frank, *J. Phys. Chem. B* **2000**, *104*, 3930.
[58] D. F. Watson, G. J. Meyer, *Coord. Chem. Rev.* **2004**, *248*, 1391.
[59] N. Papageorgiou, Y. Athanassov, M. Armand, P. Bonhote, H. Pettersson, A. Azam, M. Grätzel, *J. Electrochem. Soc.* **1996**, *143*, 3099.
[60] M. Gorlov, L. Kloo, *Dalton Trans.* **2008**, 2655.
[61] S. M. Zakeeruddin, M. Grätzel, *Adv. Funct. Mater.* **2009**, *19*, 2187.
[62] A. F. Nogueira, C. Longo, M. A. De Paoli, *Coord. Chem. Rev.* **2004**, *248*, 1455.
[63] A. J. Frank, N. Kopidakis, J. van de Lagemaat, *Coord. Chem. Rev.* **2004**, *248*, 1165.
[64] a) G. Schlichthörl, S. Y. Huang, J. Sprague, A. J. Frank, *J. Phys. Chem. B* **1997**, *101*, 8141; b) S. Pelet, J.-E. Moser, M. Grätzel, *J. Phys. Chem. B* **2000**, *104*, 1791.
[65] a) N. R. Neale, N. Kopidakis, J. van de Lagemaat, M. Grätzel, A. J. Frank, *J. Phys. Chem. B* **2005**, *109*, 23183; b) Z. Zhang, N. Evans, S. M. Zakeeruddin, R. Humphry-Baker, M. Grätzel, *J. Phys. Chem. C* **2007**, *111*, 398.
[66] K. Fredin, J. Nissfolk, G. Boschloo, A. Hagfeldt, *J. Electroanal. Chem.* **2007**, *609*, 55.
[67] H. Kusama, M. Kurashige, H. Arakawa, *J. Photochem. Photobiol., A* **2005**, *169*, 169.
[68] G. Boschloo, L. Haeggman, A. Hagfeldt, *J. Phys. Chem. B* **2006**, *110*, 13144.
[69] K.-M. Lee, V. Suryanarayanan, K.-C. Ho, K. R. J. Thomas, J. T. Lin, *Sol. Energy Mater. Sol. Cells* **2007**, *91*, 1426.
[70] T. N. Murakami, M. Grätzel, *Inorg. Chim. Acta* **2008**, *361*, 572.
[71] N. Papageorgiou, W. F. Maier, M. Grätzel, *J. Electrochem. Soc.* **1997**, *144*, 876.
[72] T. Ma, X. Fang, M. Akiyama, K. Inoue, H. Noma, E. Abe, *J. Electroanal. Chem.* **2004**, *574*, 77.

[73] T. N. Murakami, S. Ito, Q. Wang, M. K. Nazeeruddin, T. Bessho, I. Cesar, P. Liska, R. Humphry-Baker, P. Comte, P. Pechy, M. Grätzel, *J. Electrochem. Soc.* **2006**, *153*, A2255.
[74] V. N. Pitchkov, *Platinum Met. Rev.* **1996**, *40*, 181.
[75] W. P. Griffith, *Chem. Soc. Rev.* **1992**, *21*, 179.
[76] a) A. Juris, V. Balzani, F. Barigelletti, S. Campagna, P. Belser, A. Von Zelewsky, *Coord. Chem. Rev.* **1988**, *84*, 85; b) P. S. Wagenknecht, P. C. Ford, *Coord. Chem. Rev.* **2011**, *255*, 591.
[77] V. Balzani, G. Bergamini, S. Campagna, F. Puntoriero, *Top. Curr. Chem.* **2007**, *280*, 1.
[78] V. Balzani, A. Juris, M. Venturi, S. Campagna, S. Serroni, *Chem. Rev.* **1996**, *96*, 759.
[79] G. A. Crosby, *Acc. Chem. Res.* **1975**, *8*, 231.
[80] K. Kalyanasundaram, M. K. Nazeeruddin, *Chem. Phys. Lett.* **1992**, *193*, 292.
[81] H. Hofmeier, U. S. Schubert, *Chem. Soc. Rev.* **2004**, *33*, 373.
[82] M. Maestri, N. Armaroli, V. Balzani, E. C. Constable, A. M. W. C. Thompson, *Inorg. Chem.* **1995**, *34*, 2759.
[83] X.-y. Wang, A. Del Guerzo, R. H. Schmehl, *J. Photochem. Photobiol. C: Photochem. Rev.* **2004**, *5*, 55.
[84] E. A. Medlycott, G. S. Hanan, *Chem. Soc. Rev.* **2005**, *34*, 133.
[85] N. E. Tokel-Takvoryan, R. E. Hemingway, A. J. Bard, *J. Am. Chem. Soc.* **1973**, *95*, 6582.
[86] A. B. P. Lever, *Inorg. Chem.* **1990**, *29*, 1271.
[87] S. S. Fielder, M. C. Osborne, A. B. P. Lever, W. J. Pietro, *J. Am. Chem. Soc.* **1995**, *117*, 6990.
[88] P. A. Anderson, G. F. Strouse, J. A. Treadway, F. R. Keene, T. J. Meyer, *Inorg. Chem.* **1994**, *33*, 3863.
[89] F. R. Keene, *Coord. Chem. Rev.* **1997**, *166*, 121.
[90] E. C. Constable, A. Thompson, *J. Chem. Soc., Dalton Trans.* **1992**, 3467.
[91] H. Muerner, P. Belser, A. von Zelewsky, *J. Am. Chem. Soc.* **1996**, *118*, 7989.
[92] M. K. Nazeeruddin, S. M. Zakeeruddin, R. Humphry-Baker, S. I. Gorelsky, A. B. P. Lever, M. Grätzel, *Coord. Chem. Rev.* **2000**, *208*, 213.
[93] L. Spiccia, G. B. Deacon, C. M. Kepert, *Coord. Chem. Rev.* **2004**, *248*, 1329.
[94] P. A. Anderson, G. B. Deacon, K. H. Haarmann, F. R. Keene, T. J. Meyer, D. A. Reitsma, B. W. Skelton, G. F. Strouse, N. C. Thomas, J. A. Treadway, A. H. White, *Inorg. Chem.* **1995**, *34*, 6145.
[95] I. P. Evans, A. Spencer, G. Wilkinson, *J. Chem. Soc., Dalton Trans.* **1973**, 204.
[96] D. A. Freedman, J. K. Evju, M. K. Pomije, K. R. Mann, *Inorg. Chem.* **2001**, *40*, 5711.
[97] T. Doi, H. Nagamiya, M. Kokubo, K. Hirabayashi, T. Takahashi, *Tetrahedron* **2002**, *58*, 2957.
[98] F. H. Burstall, *J. Chem. Soc.* **1936**, 173.
[99] a) C. T. Lin, W. Boettcher, M. Chou, C. Creutz, N. Sutin, *J. Am. Chem. Soc.* **1976**, *98*, 6536; b) G. A. Crosby, R. J. Watts, *J. Am. Chem. Soc.* **1971**, *93*, 3184.
[100] N. C. Thomas, G. B. Deacon, *Inorg. Synth.* **1989**, *25*, 107.
[101] M. Haberecht, J. M. Schnorr, E. V. Andreitchenko, C. G. Clark, M. Wagner, K. Müllen, *Angew. Chem. Int. Ed.* **2008**, *47*, 1662.
[102] G. W. Walker, D. G. Nocera, S. Swavey, K. J. Brewer, *Inorg. Synth.* **2004**, *34*, 66.
[103] X. Xiao, J. Sakamoto, M. Tanabe, S. Yamazaki, S. Yamabe, T. Matsumura-Inoue, *J. Electroanal. Chem.* **2002**, *527*, 33.
[104] H. J. Bolink, L. Cappelli, E. Coronado, M. Grätzel, M. K. Nazeeruddin, *J. Am. Chem. Soc.* **2006**, *128*, 46.
[105] S. Rau, S. Bernhard, A. Grübing, S. Schebesta, K. Lamm, J. Vieth, H. Görls, D. Walther, M. Rudolph, U. W. Grummt, E. Birkner, *Inorg. Chim. Acta* **2004**, *357*, 4496.
[106] O. Johansson, H. Wolpher, M. Borgstrom, L. Hammarstrom, J. Bergquist, L. Sun, B. Akermark, *Chem. Commun.* **2004**, 194.
[107] D. Hesek, Y. Inoue, S. R. L. Everitt, H. Ishida, M. Kunieda, M. G. B. Drew, *Inorg. Chem.* **2000**, *39*, 308.
[108] T. J. Rutherford, D. A. Reitsma, F. R. Keene, *J. Chem. Soc., Dalton Trans.* **1994**, 3659.
[109] G. F. Strouse, P. A. Anderson, J. R. Schoonover, T. J. Meyer, F. R. Keene, *Inorg. Chem.* **1992**, *31*, 3004.
[110] G. B. Deacon, C. M. Kepert, N. Sahely, B. W. Skelton, L. Spiccia, N. C. Thomas, A. H. White, *J. Chem. Soc., Dalton Trans.* **1999**, 275.
[111] S. M. Zakeeruddin, M. K. Nazeeruddin, R. Humphry-Baker, M. Grätzel, V. Shklover, *Inorg. Chem.* **1998**, *37*, 5251.
[112] J. P. Sauvage, J. P. Collin, J. C. Chambron, S. Guillerez, C. Coudret, V. Balzani, F. Barigelletti, L. De Cola, L. Flamigni, *Chem. Rev.* **1994**, *94*, 993.
[113] D. L. Greene, D. M. P. Mingos, *Trans. Met. Chem.* **1991**, *16*, 71.
[114] R. Ziessel, V. Grosshenny, M. Hissler, C. Stroh, *Inorg. Chem.* **2004**, *43*, 4262.
[115] R. Lalrempuia, M. Rao Kollipara, *Polyhedron* **2003**, *22*, 3155.
[116] W.-S. Han, J.-K. Han, H.-Y. Kim, M. J. Choi, Y.-S. Kang, C. Pac, S. O. Kang, *Inorg. Chem.* **2011**, *50*, 3271.
[117] a) S. Ito, S. M. Zakeeruddin, R. Humphry-Baker, P. Liska, R. Charvet, P. Comte, M. K. Nazeeruddin, P. Péchy, M. Takata, H. Miura, S. Uchida, M. Grätzel, *Adv. Mater.* **2006**, *18*, 1202; b) Z.-S. Wang, H. Kawauchi, T. Kashima, H. Arakawa, *Coord. Chem. Rev.* **2004**, *248*, 1381.
[118] M. K. Nazeeruddin, A. Kay, I. Rodicio, R. Humphry-Baker, E. Mueller, P. Liska, N. Vlachopoulos, M. Grätzel, *J. Am. Chem. Soc.* **1993**, *115*, 6382.
[119] a) H. T. Nguyen, H. M. Ta, T. Lund, *Sol. Energy Mater. Sol. Cells* **2007**, *91*, 1934; b) P. Tuyet Nguyen, R. Degn, H. Thai Nguyen, T. Lund, *Sol. Energy Mater. Sol. Cells* **2009**, *93*, 1939.
[120] a) S. H. Wadman, J. M. Kroon, K. Bakker, M. Lutz, A. L. Spek, G. P. M. van Klink, G. van Koten, *Chem. Commun.* **2007**, 1907; b) T. Bessho, E. Yoneda, J.-H. Yum, M. Guglielmi, I. Tavernelli, H. Imai, U. Rothlisberger, M. K. Nazeeruddin, M. Grätzel, *J. Am. Chem. Soc.* **2009**, *131*, 5930; c) S. H. Wadman, J. M. Kroon, K. Bakker, R. W. A. Havenith, G. P. M. van Klink, G. van Koten, *Organometallics* **2010**, *29*, 1569; d) K. C. D. Robson, B. D. Koivisto, A. Yella, B. Sporinova, M. K. Nazeeruddin, T. Baumgartner, M. Grätzel, C. P. Berlinguette, *Inorg. Chem.* **2011**, *50*, 5494; e) P. G. Bomben, B. D. Koivisto, C. P. Berlinguette, *Inorg. Chem.* **2010**, *49*, 4960; f) K.-L. Wu, H.-C. Hsu, K. Chen, Y. Chi, M.-W. Chung, W.-H. Liu, P.-T. Chou, *Chem. Commun.* **2010**, *46*, 5124.
[121] a) A. Islam, H. Sugihara, L. P. Singh, K. Hara, R. Katoh, Y. Nagawa, M. Yanagida, Y. Takahashi, S. Murata, H. Arakawa, *Inorg. Chim. Acta* **2001**, *322*, 7; b) A. Kukrek, D. Wang, Y. Hou, R. Zong, R. Thummel, *Inorg. Chem.* **2006**, *45*, 10131.
[122] P. Wang, C. Klein, J.-E. Moser, R. Humphry-Baker, N.-L. Cevey-Ha, R. Charvet, P. Comte, S. M. Zakeeruddin, M. Grätzel, *J. Phys. Chem. B* **2004**, *108*, 17553.
[123] M. I. Asghar, K. Miettunen, J. Halme, P. Vahermaa, M. Toivola, K. Aitola, P. Lund, *Energy Environ. Sci.* **2010**, *3*, 418.
[124] a) S. M. Zakeeruddin, M. K. Nazeeruddin, R. Humphry-Baker, P. Péchy, P. Quagliotto, C. Barolo, G. Viscardi, M. Grätzel, *Langmuir* **2002**, *18*, 952; b) C. Klein, M. K. Nazeeruddin, D. Di Censo, P. Liska, M. Grätzel, *Inorg. Chem.* **2004**, *43*, 4216.
[125] a) R. Argazzi, C. A. Bignozzi, T. A. Heimer, F. N. Castellano, G. J. Meyer, *J. Am. Chem. Soc.* **1995**, *117*, 11815; b) N. Hirata, J.-J. Lagref, E. J. Palomares, J. R. Durrant, M. K. Nazeeruddin, M. Grätzel, D. Di Censo, *Chem. Eur. J.* **2004**, *10*, 595.
[126] M. Abrahamsson, P. G. Johansson, S. Ardo, A. Kopecky, E. Galoppini, G. J. Meyer, *J. Phys. Chem. Lett.* **2010**, 1725.
[127] a) M. K. Nazeeruddin, S. M. Zakeeruddin, R. Humphry-Baker, M. Jirousek, P. Liska, N. Vlachopoulos, V. Shklover, C.-H. Fischer, M. Grätzel, *Inorg. Chem.* **1999**, *38*, 6298; b) M. Yanagida, L. P. Singh, K. Sayama, K. Hara, R. Katoh,

A. Islam, H. Sugihara, H. Arakawa, M. K. Nazeeruddin, M. Grätzel, *J. Chem. Soc., Dalton Trans.* **2000**, 2817.
[128] B. C. O'Regan, K. Walley, M. Juozapavicius, A. Anderson, F. Matar, T. Ghaddar, S. M. Zakeeruddin, C. Klein, J. R. Durrant, *J. Am. Chem. Soc.* **2009**, *131*, 3541.
[129] A. Reynal, A. Forneli, E. Martinez-Ferrero, A. Sanchez-Diaz, A. Vidal-Ferran, B. C. O'Regan, E. Palomares, *J. Am. Chem. Soc.* **2008**, *130*, 13558.
[130] a) B. C. O'Regan, I. López-Duarte, M. V. Martínez-Díaz, A. Forneli, J. Albero, A. Morandeira, E. Palomares, T. Torres, J. R. Durrant, *J. Am. Chem. Soc.* **2008**, *130*, 2906; b) Z.-S. Wang, N. Koumura, Y. Cui, M. Miyashita, S. Mori, K. Hara, *Chem. Mater.* **2009**, *21*, 2810.

Received: May 20, 2011
Published Online: August 29, 2011

